

1 **Erosion of somatic tissue identity with loss of the X-linked**
2 **intellectual disability factor KDM5C**

3

4 Katherine M. Bonefas, Ilakkiya Venkatachalam, and Shigeki Iwase.

5 **Abstract**

6 Mutations in numerous chromatin-modifying enzymes cause neurodevelopmental disorders (NDDs). Loss
7 of repressive chromatin regulators can lead to the aberrant transcription of tissue-specific genes outside
8 of their intended context, however the mechanisms and consequences of their dysregulation are largely
9 unknown. Here, we examine the roles of the NDD-associated lysine demethylase 5c (KDM5C), an eraser of
10 histone 3 lysine 4 di and tri-methylation (H3K4me2/3), in tissue identity. We found male *Kdm5c* knockout
11 (-KO) mice, which recapitulate key behavioral phenotypes of Claes-Jensen X-linked intellectual disability,
12 aberrantly expresses many liver, muscle, ovary, and testis genes within the amygdala and hippocampus.
13 Gonad-enriched genes expressed in the *Kdm5c*-KO brain were typically unique to germ cells, indicating an
14 erosion of the soma-germline boundary. Germline genes are usually decommissioned in somatic lineages in
15 the post-implantation epiblast, yet *Kdm5c*-KO epiblast-like cells (EpiLCs) aberrantly expressed key regulators
16 of germline identity and meiosis, including *Dazl* and *Stra8*. Germline gene suppression is sexually dimorphic,
17 as female EpiLCs required a higher dose of KDM5C to maintain germline gene suppression. Using a
18 comprehensive list of mouse germline-enriched genes, we found KDM5C is selectively recruited to a subset
19 of germline gene promoters that contain CpG islands (CGIs) to facilitate DNA CpG methylation (CpGme)
20 during ESC to EpiLC differentiation. However, late stage spermatogenesis genes devoid of promoter CGIs
21 can also become activated in *Kdm5c*-KO cells via ectopic activation by RFX transcription factors. Thus,
22 distinct suppressive mechanisms are recruited to different germline gene classes and ectopic germline
23 transcriptional programs can mirror germ cell development within somatic tissues.

24 **Introduction**

25 A single genome holds the instructions to generate the myriad of cell types found within an organism.
26 This is, in part, accomplished by chromatin regulators that can either promote or impede lineage-specific
27 gene expression through DNA and histone modifications^{1–5}. Human genetic studies revealed mutations in

28 chromatin regulators are a major cause of neurodevelopmental disorders (NDDs)⁶ and many studies have
29 identified their importance for regulating brain-specific transcriptional programs. Loss of some chromatin
30 regulators can also result in the ectopic expression of tissue-specific genes outside of their target environment,
31 such as the misexpression of liver-specific genes within adult neurons⁷. However, the mechanisms underlying
32 ectopic gene expression and its impact upon neurodevelopment are poorly understood.

33 To elucidate the role of tissue identity in chromatin-linked NDDs, it is essential to first characterize the
34 nature of the dysregulated genes and the molecular mechanisms governing their de-repression. Here we
35 focus on lysine demethylase 5C (KDM5C, also known as SMCX or JARID1C), which erases histone 3 lysine
36 4 di- and trimethylation (H3K4me2/3), a permissive chromatin modification enriched at gene promoters⁸.
37 Pathogenic mutations in *KDM5C* cause Intellectual Developmental Disorder, X-linked, Syndromic, Claes-
38 Jensen Type (MRXSCJ, OMIM: 300534). MRXSCJ is more common and severe in males and its neurological
39 phenotypes include intellectual disability, seizures, aberrant aggression, and autistic behaviors^{9–11}. Male
40 *Kdm5c* knockout (-KO) mice recapitulate key MRXSCJ phenotypes, including hyperaggression, increased
41 seizure propensity, and learning impairments^{12,13}. RNA sequencing (RNA-seq) of the *Kdm5c*-KO hippocam-
42 pus revealed ectopic expression of some germline genes within the brain¹³. However, it is unclear if other
43 tissue-specific genes are aberrantly transcribed with KDM5C loss, at what point in development germline
44 gene misexpression begins, and what mechanisms underlie their dysregulation.

45 Distinguishing between germ cells and somatic cells is a key feature of multicellularity¹⁴ that occurs
46 during early embryogenesis in many metazoans¹⁵. In mammals, chromatin regulators are crucial for
47 decommissioning germline genes during the transition from naïve to primed pluripotency. Initially, germline
48 gene promoters gain repressive histone H2A lysine 119 monoubiquitination (H2AK119ub1)¹⁶ and histone 3
49 lysine 9 trimethylation (H3K9me3)^{16,17} in embryonic stem cells (ESCs) and are then decorated with DNA
50 CpG methylation (CpGme) in the post-implantation embryo^{17–19}. The contribution of KDM5C to this process
51 remains unclear. Furthermore, studies on germline gene repression have primarily been conducted in males
52 and focused on marker genes important for germ cell development rather than germline genes as a whole,
53 given the lack of a curated list for germline-enriched genes. Therefore, it is unknown if the mechanism
54 of repression differs between sexes or for certain classes of germline genes, e.g. meiotic genes versus
55 spermatid differentiation genes.

56 To illuminate KDM5C's role in tissue identity, here we characterized the aberrant expression of tissue-
57 enriched genes within the *Kdm5c*-KO brain and epiblast-like stem cells (EpiLCs), an *in vitro* model of the
58 post-implantation embryo. We curated list of mouse germline-enriched genes, which enabled genome-wide
59 analysis of germline gene silencing mechanisms for the first time. Based on the data presented below, we
60 propose KDM5C plays a fundamental, sexually dimorphic role in the development of tissue identity during
61 early embryogenesis, including the establishment of the soma-germline boundary.

62 **Results**

63 **Tissue-enriched genes are aberrantly expressed in the *Kdm5c*-KO brain**

64 Previous RNA sequencing (RNA-seq) of the adult male *Kdm5c*-KO hippocampus revealed ectopic
65 expression of some germline genes unique to the testis¹³. It is currently unknown if the testis is the only
66 tissue type misexpressed in the *Kdm5c*-KO brain. We systematically tested whether other tissue-specific
67 genes are misexpressed in the brain with constitutive knockout of *Kdm5c*²⁰ by using a published list of mouse
68 tissue-enriched genes²¹.

69 We found a large proportion of significantly upregulated genes (DESeq2²², log2 fold change > 0.5, q
70 < 0.1) within the male *Kdm5c*-KO brain are typically enriched within non-brain tissues (Amygdala: 35%,
71 Hippocampus: 24%) (Figure 1A-B). For both the amygdala and hippocampus, the majority of tissue-enriched
72 differentially expressed genes (DEGs) were testis genes (Figure 1A-C). Even though the testis has the
73 largest total number of tissue-biased genes (2,496 genes) compared to any other tissue, testis-biased DEGs
74 were significantly enriched for both brain regions (Amygdala p = 1.83e-05, Odds Ratio = 5.13; Hippocampus
75 p = 4.26e-11, Odds Ratio = 4.45, Fisher's Exact Test). One example of a testis-enriched gene misexpressed
76 in the *Kdm5c*-KO brain is *FK506 binding protein 6* (*Fkbp6*), a known regulator of PIWI-interacting RNAs
77 (piRNAs) and meiosis^{23,24} (Figure 1C).

78 Interestingly, we also observed significant enrichment of ovary-biased DEGs in both the amygdala and
79 hippocampus (Amygdala p = 0.00574, Odds Ratio = 18.7; Hippocampus p = 0.048, Odds Ratio = 5.88,
80 Fisher's Exact) (Figure 1A-B). Ovary-enriched DEGs included *Zygotic arrest 1* (*Zar1*), which sequesters
81 mRNAs in oocytes for meiotic maturation²⁵ (Figure 1D). Given that the *Kdm5c*-KO mice we analyzed are
82 male, these data demonstrate that the ectopic expression of gonad-enriched genes is independent of
83 organismal sex.

84 Although not consistent across brain regions, we also found significant enrichment of DEGs biased
85 towards two non-gonadal tissues - the liver (Amygdala p = 0.04, Odds Ratio = 6.58, Fisher's Exact Test) and
86 the muscle (Hippocampus p = 0.01, Odds Ratio = 6.95, Fisher's Exact Test) (Figure 1A-B). *Apolipoprotein*
87 *C-1* (*Apoc1*) a lipoprotein metabolism and transport gene, is among the liver-biased DEG derepressed in both
88 the hippocampus and amygdala²⁶ and its brain overexpression has been implicated in Alzheimer's disease²⁷
89 (Figure 1E).

90 For all *Kdm5c*-KO tissue-enriched DEGs, aberrantly expressed mRNAs are polyadenylated and spliced
91 into mature transcripts (Figure 1C-E). Of note, we observed little to no dysregulation of brain-enriched genes
92 (Amygdala p = 1, Odds Ratio = 1.22; Hippocampus p = 0.74, Odds Ratio = 1.22, Fisher's Exact), despite the
93 fact these are brain samples and the brain has the second highest total number of tissue-enriched genes
94 (708 genes). Altogether, these results suggest the aberrant expression of tissue-enriched genes within the
95 brain is a major effect of KDM5C loss.

96 **Germline genes are misexpressed in the *Kdm5c*-KO brain**

97 *Kdm5c*-KO brain expresses testicular germline genes¹³, however the testis also contains somatic cells that
98 support hormone production and germline functions. To determine if *Kdm5c*-KO results in ectopic expression
99 of somatic testicular genes, we first evaluated the known functions of testicular DEGs through gene ontology.
100 We found *Kdm5c*-KO testis-enriched DEGs had high enrichment of germline-relevant ontologies, including
101 spermatid development (GO: 0007286, p.adjust = 6.2e-12) and sperm axoneme assembly (GO: 0007288,
102 p.adjust = 2.45e-14) (Figure 2A).

103 We then evaluated testicular DEG expression in wild-type testes versus testes with germ cell depletion²⁸,
104 which was accomplished by heterozygous *W* and *Wv* mutations in the enzymatic domain of *c-Kit* (*Kit*^{W/Wv})²⁹.
105 Almost all *Kdm5c*-KO testis-enriched DEGs lost expression with germ cell depletion (Figure 2B). We then
106 assessed testis-enriched DEG expression in a published single cell RNA-seq dataset that identified cell
107 type-specific markers within the testis³⁰. Some *Kdm5c*-KO testis-enriched DEGs were classified as specific
108 markers for different germ cell developmental stages (e.g. spermatogonia, spermatocytes, round spermatids,
109 and elongating spermatids), yet none marked somatic cells (Figure 2C). Together, these data demonstrate
110 that the *Kdm5c*-KO brain aberrantly expresses germline genes, but not somatic testicular genes, reflecting
111 an erosion of the soma-germline boundary.

112 As of yet, research on germline gene silencing mechanisms has focused on a handful of key genes
113 rather than assessing germline gene suppression genome-wide due to the lack of a comprehensive gene list.
114 We therefore generated a list of mouse germline-enriched genes using RNA-seq datasets of *Kit*^{W/Wv} mice
115 that included males and females at embryonic day 12, 14, and 16³¹ and adult male testes²⁸. We defined
116 genes as germline-enriched if their expression met the following criteria: 1) their expression is greater than
117 1 FPKM in wild-type gonads 2) their expression in any non-gonadal tissue of adult wild type mice²¹ does
118 not exceed 20% of their maximum expression in the wild-type germline, and 3) their expression in the germ
119 cell-depleted gonads, for any sex or time point, does not exceed 20% of their maximum expression in the
120 wild-type germline. These criteria yielded 1,288 germline-enriched genes (Figure 2D), which was hereafter
121 used as a resource to globally characterize germline gene misexpression with *Kdm5c* loss (Supplementary
122 table 1).

123 ***Kdm5c*-KO epiblast-like cells aberrantly express key regulators of germline identity**

124 Germ cells are typically distinguished from somatic cells soon after the embryo implants into the uterine
125 wall^{32,33}, when germline genes are silenced in epiblast stem cells that will form the somatic tissues³⁴. This
126 developmental time point can be modeled *in vitro* through differentiation of naïve embryonic stem cells
127 (nESCs) into epiblast-like stem cells (EpiLCs) (Figure 3A)^{35,36}. While some germline-enriched genes are
128 also expressed in nESCs and in the 2-cell stage³⁷⁻³⁹, they are silenced as they differentiate into EpiLCs^{17,40}.
129 Therefore, we tested if KDM5C was necessary for the initial silencing of germline genes in somatic lineages

130 by evaluating the impact of *Kdm5c* loss in male EpiLCs.

131 *Kdm5c*-KO cell morpholgy during ESC to EpiLC differentiation appeared normal (Figure 3B) and EpiLCs
132 properly expressed markers of primed pluripotency, such as *Dnmt3b*, *Fgf5*, *Pou3f1*, and *Otx2* (Figure 3C). We
133 then identified tissue-enriched DEGs in a RNA-seq dataset of wild-type and *Kdm5c*-KO EpiLCs⁴¹ (DESeq2,
134 log2 fold change > 0.5, q < 0.1). Similar to the *Kdm5c*-KO brain, we observed general dysregulation of
135 tissue-enriched genes, with the largest number of genes belonging to the brain and testis, although they
136 were not significantly enriched (Figure 3D). Using our list of mouse germline-enriched genes assembled
137 above, we found 68 germline genes were misexpressed in male *Kdm5c*-KO EpiLCs.

138 We then compared EpiLC germline DEGs to those expressed in the *Kdm5c*-KO brain to determine if
139 germline genes are constitutively dysregulated or change over the course of development. The majority of
140 germline DEGs were unique to either EpiLCs or the brain, with only *D1Pas1* and *Cyct* shared across all
141 tissue/cell types (Figure 3E-F). EpiLCs had particularly high enrichment of meiosis-related gene ontologies
142 (Figure 3G), such as meiotic cell cycle process (GO:1903046, p.adjust = 2.2e-07) and meiotic nuclear
143 division (GO:0140013, p.adjust = 1.37e-07). While there was modest enrichment of meiotic gene ontologies
144 in both brain regions, the *Kdm5c*-KO hippocampus primarily expressed late-stage spermatogenesis genes
145 involved in sperm axoneme assembly (GO:0007288, p.adjust = 0.00621) and sperm motility (GO:0097722,
146 p.adjust = 0.00612).

147 Notably, DEGs unique to *Kdm5c*-KO EpiLCs included key drivers of germline identity, such as *Stimulated*
148 *by retinoic acid 8* (*Stra8*: log2 fold change = 3.73, q = 2.17e-39) and *Deleted in azoospermia like* (*Dazl*):
149 log2 fold change = 3.36, q = 3.19e-12) (Figure 3H). These genes are typically expressed when primordial
150 germ cells (PGCs) are committed to the germline fate and later in life to trigger meiotic gene expression
151 programs⁴²⁻⁴⁴. Of note, some germline genes, including *Dazl*, are also expressed in the two-cell embryo^{38,45}.
152 However, we did not see derepression of two-cell stage-specific genes, like *Duxf3* (*Dux*) (log2 fold change
153 = -0.282, q = 0.337) and *Zscan4d* (log2 fold change = 0.25, q = 0.381) (Figure 3H), indicating *Kdm5c*-KO
154 EpiLCs do not revert back to a 2-cell state. Altogether, *Kdm5c*-KO EpiLCs express key drivers of germline
155 identity and meiosis while the brain primarily expresses spermiogenesis genes, indicating germline gene
156 misexpression mirrors germline development during the progression of somatic development.

157 **Female epiblast-like cells have increased sensitivity to germline gene misexpression 158 with *Kdm5c* loss**

159 It is currently unknown if the misexpression of germline genes is influenced by sex, as previous studies
160 on germline gene repressors have focused on male cells^{16-18,46,47}. Sex is particularly pertinent in the case
161 of KDM5C because it partially escapes X chromosome inactivation (XCI), resulting in a higher dosage in
162 females⁴⁸⁻⁵¹. We therefore explored the impact of chromosomal sex upon germline gene suppression by
163 comparing their dysregulation in male *Kdm5c* hemizygous knockout (XY *Kdm5c*-KO), female homozygous

164 knockout (XX *Kdm5c*-KO), and female heterozygous knockout (XX *Kdm5c*-HET) EpiLCs.⁴¹.
165 Homozygous and heterozygous *Kdm5c* knockout females expressed over double the number of germline-
166 enriched genes than hemizygous males (Figure 4A). While the majority of germline DEGs in *Kdm5c*-KO
167 males were also dysregulated in females (74%), many were sex-specific, such as *Tktl2* and *Esx1* (Figure
168 4B). We then compared the known functions of germline genes dysregulated only in females (XX only -
169 dysregulated in XX *Kdm5c*-KO, XX *Kdm5c*-HET, or both), only in males (XY only), or in all samples (shared)
170 (Figure 4C). Female-specific germline DEGs were enriched for meiotic (GO:0051321 meiotic cell cycle) and
171 flagellar (GO:0003341 cilium movement) functions, while male-specific DEGs had roles in mitochondrial
172 and cell signaling (GO:0070585 protein localization to mitochondrion). Germline transcripts expressed in
173 both sexes were enriched for meiotic (GO:0140013 meiotic nuclear division) and egg-specific functions
174 (GO:0007292 female gamete generation).

175 The majority of germline genes expressed in both sexes were more highly dysregulated in females
176 compared to males (Figure 4D-F). This increased degree of dysregulation in females, along with the
177 increased total number of germline genes, indicates females are more sensitive to losing KDM5C-mediated
178 germline gene suppression. Female sensitivity could be due to impaired XCI in *Kdm5c* mutants⁴¹, as many
179 spermatogenesis genes lie on the X chromosome^{52,53}. However, female germline DEGs were not biased
180 towards the X chromosome and had a similar overall proportion of X chromosome DEGs compared to
181 males (XY *Kdm5c*-KO - 10.29%, XX *Kdm5c*-HET - 7.43%, XX *Kdm5c*-KO - 10.59%) (Figure 4G). The
182 majority of germline DEGs instead lie on autosomes for both male and female *Kdm5c* mutants (Figure 4G).
183 Thus, while female EpiLCs are more prone to germline gene misexpression with KDM5C loss, it is likely
184 independent of XCI defects.

185 **Germline gene misexpression in *Kdm5c* mutants is independent of germ cell sex**

186 Although many germline genes have shared functions in the male and female germline, some have
187 unique or sex-biased expression. Therefore, we wondered if *Kdm5c* mutant males would primarily express
188 sperm genes while mutant females primarily expressed egg genes. To comprehensively assess whether
189 germline gene sex corresponds with *Kdm5c* mutant sex, we first filtered our list of germline-enriched genes
190 for egg and sperm-biased genes (Figure 4H). We defined germ cell sex-biased genes as those whose
191 expression in the opposite sex, at any time point, is no greater than 20% of the gene's maximum expression
192 in a given sex. This yielded 67 egg-biased, 1,024 sperm-biased, and 197 unbiased germline-enriched genes.
193 We found egg, sperm, and unbiased germline genes were dysregulated in all *Kdm5c* mutants at similar
194 proportions (Figure 4I-J). Furthermore, germline genes dysregulated exclusively in either male or female
195 mutants were also not biased towards their corresponding germ cell sex (Figure 4I). Altogether, these results
196 demonstrate sex differences in germline gene dysregulation is not due to sex-specific activation of sperm or
197 egg transcriptional programs.

198 **KDM5C binds to a subset of germline gene promoters during early embryogenesis**

199 KDM5C binds to the promoters of several germline genes in embryonic stem cells (ESCs) but its binding
200 is absent in neurons¹³. However, the lack of a comprehensive list of germline-enriched genes prohibited
201 genome-wide characterization of KDM5C binding at germline gene promoters. Thus, it is unclear if KDM5C
202 is enriched at germline gene promoters, what types of germline genes KDM5C regulates, and if its binding is
203 maintained at any germline genes in neurons.

204 To address these questions, we analyzed KDM5C chromatin immunoprecipitation followed by DNA
205 sequencing (ChIP-seq) datasets in EpiLCs⁴¹ and primary forebrain neuron cultures (PNCs)¹². EpiLCs had a
206 higher total number of high-confidence KDM5C peaks than PNCs (EpiLCs: 5,808, PNCs: 1,276, MACS2 q <
207 0.1 and fold enrichment > 1). KDM5C was primarily localized to gene promoters in both cell types (EpiLCs:
208 4,190, PNCs: 745 ± 500bp from the TSS), although PNCs showed increased localization to non-promoter
209 regions (Figure 5A).

210 The majority of promoters bound by KDM5C in PNCs were also bound in EpiLCs (513 shared promoters),
211 however a large portion of gene promoters were bound by KDM5C only in EpiLCs (3,677 EpiLC only
212 promoters) (Figure 5B). Genes bound by KDM5C in both PNCs and EpiLCs were enriched for functions
213 involving nucleic acid turnover, such as deoxyribonucleotide metabolic process (GO:0009262, p.adjust =
214 8.28e-05) (Figure 5C). Germline-specific ontologies were enriched only in EpiLC-specific KDM5C-bound
215 promoters, such as meiotic nuclear division (GO: 0007127 p.adjust = 6.77e-16) (Figure 5C). There were no
216 ontologies significantly enriched for PNC-specific KDM5C target genes. Using our mouse germline gene list,
217 we observed evident KDM5C signal around the TSS of many germline genes in EpiLCs, but not in PNCs
218 (Figure 5D). Based on our ChIP-seq peak cut-off criteria, KDM5C was highly enriched at 211 germline gene
219 promoters in EpiLCs (16.4% of all germline genes) (Figure 5E). Of note, KDM5C was only bound to about
220 one third of *Kdm5c*-KO RNA-seq DEG promoters (EpiLC only DEGs: 34.92063%, Brain only DEGs: 30%)
221 (Supplementary figure 1A-C). However, KDM5C did bind the promoter of 4 out of the 5 genes dysregulated
222 in both the brain and EpiLCs. Representative examples of KDM5C-bound and unbound germline DEGs
223 are *Dazl* and *Stra8*, respectively (Figure 5F). Together, these results demonstrate KDM5C is recruited to a
224 subset of germline genes in EpiLCs, including meiotic genes, but does not directly regulate germline genes
225 in neurons. Furthermore, the majority of germline mRNAs expressed in *Kdm5c*-KO cells are dysregulated
226 independent of direct KDM5C binding to their promoters.

227 Many germline-specific genes are suppressed by the polycomb repressive complex 1.6 (PRC1.6), which
228 contains transcription factor heterodimers E2F6/DP1 and MGA/MAX that respectively bind E2F and E-box
229 motifs⁵⁶. PRC1.6 members may recruit KDM5C to germline gene promoters, given their association with
230 KDM5C in HeLa cells and ESCs^{45,57}. We thus used HOMER⁵⁸ to identify transcription factor motifs enriched
231 at KDM5C-bound or unbound germline gene promoters (TSS ± 500 bp, q-value < 0.1). MAX and E2F6 binding
232 sites were significantly enriched at germline genes bound by KDM5C in EpiLCs (MAX q-value: 0.0068, E2F6
233 q-value: 0.0673, E2F q-value: 0.0917), but not at germline genes unbound by KDM5C (Figure 5G). One third

234 of KDM5C-bound promoters contained the consensus sequence for either E2F6 (E2F, 5'-TCCCGC-3'), MGA
235 (E-box, 5'-CACGTG-3'), or both, but only 17% of KDM5C-unbound genes contained these motifs (Figure
236 5H). KDM5C-unbound germline genes were instead enriched for multiple RFX transcription factor binding
237 sites (RFX q-value < 0.0001, RFX2 q-value < 0.0001, RFX5 q-value < 0.0001) (Figure 5I, Supplementary
238 figure 1D). RFX transcription factors bind X-box motifs⁵⁹ to promote ciliogenesis^{60,61} and among them is
239 RFX2, a central regulator of post-meiotic spermatogenesis^{62,63}. Interestingly, RFX2 mRNA is derepressed
240 in *Kdm5c*-KO EpiLCs (Figure 5J), however it is also not a direct target of KDM5C (Supplementary figure
241 1E). Thus, RFX2 is a candidate transcription factor for driving the ectopic expression of KDM5C-unbound
242 germline genes in *Kdm5c*-KO cells.

243 **KDM5C is recruited to CpG islands within germline gene promoters to facilitate *de*
244 *novo* DNA methylation**

245 In the early embryo, germline gene promoters are initially decorated with repressive histone modifications
246 and are then silenced long-term via DNA CpG methylation (CpGme)^{16,17,40,64}. Our results above indicate
247 KDM5C also acts at germline gene promoters during this time period. However, how KDM5C interacts with
248 other germline gene silencing mechanisms is currently unclear. KDM5C is generally thought to suppress
249 transcription through erasure of histone 3 lysine 4 di- and trimethylation (H3K4me2/3)⁸, yet KDM5C's
250 catalytic activity was recently shown to be dispensable for suppressing *Dazl* in undifferentiated ESCs⁴⁵. Since
251 H3K4me3 impedes *de novo* CpGme placement^{65,66}, KDM5C's catalytic activity may instead be required
252 in the post-implantation embryo for long-term silencing of germline genes. In support of this, CpGme is
253 markedly reduced at two germline gene promoters in the *Kdm5c*-KO adult hippocampus¹³.

254 Based on the above observations, we hypothesized KDM5C erases H3K4me3 to promote the initial
255 placement of CpGme at germline gene promoters in EpiLCs. To test this hypothesis, we first characterized
256 KDM5C's substrates (H3K4me2/3) at germline gene promoters in our published ChIP-seq datasets of male
257 wild-type and *Kdm5c*-KO amygdala²⁰ and EpiLCs⁴¹. In congruence with the *Kdm5c*-KO hippocampus¹³,
258 we observed aberrant accumulation of H3K4me3 around the TSS of germline genes in the *Kdm5c*-KO
259 amygdala (Figure 6A). There was also a marked increase in H3K4me2 around the TSS of germline genes
260 in *Kdm5c*-KO EpiLCs (Figure 6B). To elucidate KDM5C's embryonic role, we then characterized KDM5C's
261 mRNA and protein expression during male ESC to EpiLC differentiation (Figure 6C). While *Kdm5c* mRNA
262 steadily decreased from 0 to 48 hours of differentiation (Figure 6D), KDM5C protein initially increased from
263 0 to 24 hours but then decreased to near knockout levels by 48 hours (Figure 6E). Together, these data
264 suggest KDM5C acts during the transition between ESCs and EpiLCs to remove H3K4me at germline gene
265 promoters.

266 Germline genes accumulate CpG methylation (CpGme) at CpG islands (CGIs) during the transition from
267 naïve to primed pluripotency^{19,40,67}, reaching peak methylation levels when differentiated into EpiLCs for 96

268 hours (extended EpiLCs, exEpiLCs)¹⁷. We first identified how many germline genes contained CGIs using
269 the UCSC genome browser⁶⁸, which classified CGIs as regions that have greater than 50% GC content, are
270 larger than 200 base pairs, and the ratio of CG dinucleotides observed over the expected amount based
271 on the number of Gs and Cs is greater than 0.6. Out of 1,288 germline-enriched genes, only 356 (27.64%)
272 had promoter CGIs (TSS ± 500 bp) (Figure 6F). CGI-containing germline genes were enriched for meiotic
273 gene ontologies, including meiotic nuclear division (GO:XXXX, p.adj) and meiosis I (GO:XXXX, p.adj) when
274 compared to CGI-free genes (Figure 6G). Although a minor portion of germline gene promoters contained
275 CGIs, CGIs strongly determined KDM5C's recruitment to germline genes (FISHER'S XXXX), with 79.15% of
276 KDM5C-bound germline genes containing CGIs (Figure 6G).

277 To assess how KDM5C loss impacts initial CpGme placement at germline gene promoters, we performed
278 whole genome bisulfite sequencing (WGBS) in male wild-type and *Kdm5c*-KO ESCs and 96 hour extended
279 EpiLCs (exEpiLCs) (Figure 6H). We first identified which germline gene promoters significantly gained
280 CpGme in wild-type cells during nESC to exEpiLCs differentiation (methylKit⁶⁹, q < 0.01, |methylation
281 difference| >= 25%, TSS ± 500 bp). In wild-type cells, the majority of germline genes gained substantial
282 CpGme at their promoter during differentiation (60.08%), regardless if their promoter contained a CGI (Figure
283 6I).

284 We then identified germline gene promoters differentially methylated in wild-type versus *Kdm5c*-KO
285 exEpiLCs (methylKit, q < 0.01, |methylation difference| > 25%, TSS ± 500 bp) and found 28 germline
286 promoters were significantly hypomethylated with *Kdm5c* loss (Figure 6J). Approximately half of germline
287 promoters hypomethylated in *Kdm5c*-KO exEpiLCs are direct targets of KDM5C in EpiLCs (13 out of 28
288 hypomethylated DMRs). Promoters that showed the most robust loss of CpGme (low q-values) harbored
289 CGIs (Figure 6J).

290 We then compared average percent CpGme at germline gene promoters with or without CGIs. While
291 the degree of CpGme was largely unchanged for non-CGI promoters, CGI promoters on average had a
292 significant reduction in CpGme with KDM5C loss (Figure 6K) (Non-CGI promoters p = 0.0846, CGI promoters
293 p = 0.0081, Mann-Whitney U test). Significantly hypomethylated promoters included genes consistently
294 dysregulated across multiple *Kdm5c*-KO RNA-seq datasets¹³, such as *Naa11* and *D1PAs1* (methylation
295 difference = -60.03%, q-value = 3.26e-153) (Figure 6L). Surprisingly, we found only a modest reduction in
296 CpGme at *Dazl*'s promoter (methylation difference = -6.525%, q-value = 0.0159) (Figure 6M). Altogether,
297 these results demonstrate KDM5C is recruited to germline gene CGIs to promote CpGme at germline gene
298 promoters during early embryogenesis, however some loci can compensate for KDM5C loss through other
299 silencing mechanisms, even when retaining H3K4me.

300 **Discussion**

301 In the above study, we demonstrate KDM5C's pivotal role in the development of tissue identity. We
302 first characterized tissue-enriched genes expressed within the *Kdm5c*-KO brain and identified substantial
303 dysregulation of testis, liver, muscle, and ovary-enriched genes. Testis genes significantly enriched within
304 the *Kdm5c*-KO amygdala and hippocampus are specific to the germline and not expressed within somatic
305 cells. *Kdm5c*-KO epiblast-like cells (EpiLCs) aberrantly express key drivers of germline identity and meiosis,
306 including *Dazl* and *Stra8*, while the adult brain primarily expresses genes important for late spermatogenesis.
307 We demonstrated that although *Kdm5c* mutant sex did not influence whether sperm or egg-specific genes
308 were misexpressed, female EpiLCs are more sensitive to germline gene de-repression. Germline genes
309 can become aberrantly expressed in *Kdm5c*-KO cells via an indirect mechanism, such as activation via
310 ectopic RFX transcription factors. Finally, we found KDM5C is dynamically regulated during ESC to EpiLC
311 differentiation to promote long-term germline gene silencing through DNA methylation at CpG islands.
312 Therefore, we propose KDM5C plays a fundamental role in the development of tissue identity during
313 early embryogenesis, including the establishment of the soma-germline boundary. By systematically
314 characterizing KDM5C's role in germline gene repression, including its interaction with known silencing
315 mechanisms, we unveiled repressive mechanisms governing distinct classes of germline gene in somatic
316 lineages. Furthermore, these data provide molecular footholds which can be exploited to test the overarching
317 contribution of ectopic germline gene expression upon neurodevelopment.

318 Although eggs and sperm employ the same transcriptional programs for shared functions, e.g. PGC
319 formation, meiosis, and genome defense, some germline genes are sex specific. We found *Kdm5c* mutant
320 males and females expressed both sperm and egg-biased genes, indicating the mechanism of derepression
321 is independent of a given germline gene's sex. However, organismal sex did greatly influence the degree of
322 germline gene dysregulation, as female *Kdm5c*-KO EpiLCs had over double the number of germline-enriched
323 DEGs compared to males. The lack of X-linked gene enrichment in females suggests that this greater
324 sensitivity to germline gene misexpress is not due to XCI defects previously reported in *Kdm5c*-KO females⁴¹.
325 Sex differences in germline gene suppression may be a consequence of females having a higher dose of
326 KDM5C than males, due to its escape from XCI^{48–51}. Intriguingly, females with heterozygous loss of *Kdm5c*
327 also had over double the number of germline DEGs than hemizygous knockout males, even though their
328 level of KDM5C should be roughly equivalent to that of wild-type males. Altogether, these results suggests
329 germline gene silencing mechanims differ between males and females, which warrants further study to
330 identify the biological implications and underlying mechanisms.

331 It is important to note that while we highlighted KDM5C's regulation of germline genes, some germline-
332 enriched genes are also expressed at the 2-cell stage and in naïve ESCs for their role in pluripotency and
333 self-renewal^{39,45,70,71}. For example, while *Dazl* is primarily known for regulating the translation of germline-
334 specific mRNAs, it is also expressed at the 2-cell stage⁷¹, in naïve ESCs³⁷, and in the inner cell mass³⁷.

335 KDM5C was thought to promote the 2-cell-to-ESC transition, given *Dazl* and *Zscan4c* are de-repressed
336 in *Kdm5c*-KO ESCs⁴⁵. Although expressed in naïve ESCs, “self-renewal” germline genes like *Dazl* are
337 silenced during ESC differentiation into epiblast stem cells/EpiLCs^{17,40}. We found that while *Kdm5c*-KO
338 EpiLCs also express *Dazl*, they did not express 2-cell-specific genes. These data suggest the 2-cell-like
339 state observed in *Kdm5c*-KO ESCs likely reflects KDM5C’s primary role in germline gene repression.
340 Germline gene misexpression in *Kdm5c*-KO EpiLCs may indicate they are differentiating into primordial germ
341 cell-like cells (PGCLCs), rather than de-differentiating into 2-cell-like cells^{32,33,35}. Yet, *Kdm5c*-KO EpiLCs
342 had normal cellular morphology and properly expressed markers for primed pluripotency, including *Otx2*
343 which is known to repress EpiLC differentiation into PGCs/PGCLCs⁷². In addition to unimpaired EpiLC
344 differentiation, *Kdm5c*-KO gross brain morphology is overall normal¹² and hardly any brain-specific genes
345 were significantly dysregulated. Thus, ectopic germline gene expression occurs in parallel with proper
346 *Kdm5c*-KO differentiation and somatic development.

347 While promoter CGIs are typically resistant to CpGme⁷³, CGIs at germline promoters are highly methylated in somatic cells⁷⁴. In EpiLCs, loss of KDM5C binding at a subset of germline gene promoters,
348 e.g. *D1Pas1* and *Naa11*, strongly impaired CGI methylation, which resulted in their long-lasting de-repression
349 into adulthood. Removal of H3K4me2/3 at CGIs is a plausible mechanism for KDM5C-mediated germline
350 gene suppression^{13,75}, given H3K4me2/3 primarily do not colocalize with CpGme⁷⁴ and can oppose DNMT3
351 activity^{65,66}. However, emerging work indicates many histone-modifying enzymes have non-catalytic functions that influence gene expression, sometimes even more potently than their catalytic roles^{76,77}. Indeed,
352 KDM5C’s catalytic activity was recently found to be dispensable for repressing *Dazl* in ESCs⁴⁵. In our study,
353 *Dazl*’s promoter still gained CpGme in *Kdm5c*-KO exEpiLCs, even with elevated H3K4me2. *Dazl* and a few
354 other germline gene CGIs use multiple repressive mechanisms to facilitate CpGme^{16,17,46,47}. Together, this
355 suggests alternative silencing mechanisms are sufficient to recruit DNMT3s to some germline CGIs, while
356 others may require KDM5C-mediated H3K4me removal to overcome promoter CGI escape from CpGme.
357 Furthermore, these results indicate the requirement for catalytic activity for the same class of genes can
358 change depending upon the locus and developmental stage.

361 By generating a comprehensive list of mouse germline-enriched genes, we were able to reveal distinct
362 repressive mechanisms governing early versus late-stage germline developmental programs. In EpiLCs,
363 KDM5C was highly enriched at germline promoters containing CGIs, many of which had roles in early
364 germ cell formation and meiosis. However, over 70% of germline-enriched gene promoters lacked CGIs,
365 including the many KDM5C-unbound germline genes that were de-repressed in *Kdm5c*-KO cells. CGI-free,
366 KDM5C-unbound germline genes were primarily late-stage spermatogenesis genes and significantly
367 enriched for RFX2 binding sites, a central regulator of spermiogenesis^{62,63}. These data suggest that once
368 activated during early embryogenesis, drivers of germline identity like *Rfx2* and *Dazl* turn on downstream
369 germline programs that can loosely mimic germ cell development, ultimately culminating in the expression of
370 spermiogenesis genes in the adult *Kdm5c*-KO brain. Therefore, we propose KDM5C is recruited to germline

371 genes that shape germ cell formation via their promoter CGIs to act as break against runaway activation of
372 germline-specific programs. Therefore, we propose KDM5C is recruited via promoter CGIs to genes that
373 shape germ cell formation and acts as break against runaway activation of germline-specific programs.

374 The above work provides the mechanistic foundation for KDM5C-mediated repression of tissue and
375 germline-specific genes. However, the contribution of these ectopic, tissue-specific genes towards *Kdm5c*-
376 KO neurological impairments is still unknown. In addition to germline genes, we also identified significant
377 enrichment of muscle, liver, and even ovary-biased transcripts within the male *Kdm5c*-KO brain. Intriguingly,
378 select liver and muscle-biased DEGs do have known roles within the brain, such as the liver-enriched lipid
379 metabolism gene *Apolipoprotein C-I (Apoc1)*²⁶. *APOC1* dysregulation is implicated in Alzheimer's disease in
380 humans²⁷ and overexpression of *Apoc1* in the mouse brain can impair learning and memory⁷⁸. KDM5C may
381 therefore be crucial for neurodevelopment by fine-tuning the expression of tissue-enriched, dosage-sensitive
382 genes like *Apoc1*. Given germline genes have no known functions within the brain, their impact upon
383 neurodevelopment is currently unknown. Ectopic testicular germline transcripts have been observed in a
384 variety of cancers^{79,80}, including brain tumors in *Drosophila* and mammals^{81,82}, indicating their dysregulation
385 may promote genome instability and cellular de-differentiation. Intriguingly, some models for other chromatin-
386 linked neurodevelopmental disorders also display impaired soma-germline demarcation^{7,83-86}. Like KDM5C,
387 the chromatin regulators underlying these conditions - DNA methyltransferase 3b (DNMT3B), H3K9me1/2
388 methyltransferases G9A/GLP, methyl-CpG -binding protein 2 (MECP2) - primarily silence gene expression.
389 Thus, KDM5C is among a growing cohort of chromatin-linked neurodevelopmental disorders with similar
390 erosion of the germline versus soma boundary. Further research is required to determine the impact of these
391 germline genes and the extent to which this phenomenon occurs in humans.

392 Materials and Methods

393 Classifying tissue-enriched and germline-enriched genes

394 Tissue-enriched differentially expressed genes (DEGs) were determined by their classification in a previ-
395 ously published dataset from 17 male and female mouse tissues²¹. This study defined tissue expression as
396 greater than 1 Fragments Per Kilobase of transcript per Million mapped read (FPKM) and tissue enrichment
397 as at least 4-fold higher expression than any other tissue.

398 We curated a list of germline-enriched genes using an RNA-seq dataset from wild-type and germline-
399 depleted (*Kit^{W/Wv}*) male and female mouse embryos from embryonic day 12, 14, and 16³¹, as well as adult
400 male testes²⁸. Germline-enriched genes met the following criteria: 1) their expression is greater than 1
401 FPKM in wild-type germline 2) their expression in any wild-type somatic tissues²¹ does not exceed 20%
402 of maximum expression in wild-type germline, and 3) their expression in the germ cell-depleted (*Kit^{W/Wv}*)
403 germline, for any sex or time point, does not exceed 20% of maximum expression in wild-type germline.

404 **Cell culture**

405 We utilized our previously established cultures of male wild-type and *Kdm5c* knockout (-KO) embryonic
406 stem cells⁴¹. Sex was confirmed by genotyping *Uba1/Uba1y* on the X and Y chromosomes with the following
407 primers: 5'-TGGATGGTGTGCCAATG-3', 5'-CACCTGCACGTTGCCCT-3'. Deletion of *Kdm5c* was
408 confirmed through the primers 5'-ATGCCCATATTAAGAGTCCTG-3', 5'-TCTGCCTTGATGGGACTGTT-3',
409 and 5'-GGTTCTAACACTCACATAGTG-3'.

410 Embryonic stem cells (ESCs) and epiblast-like cells were cultured using previously established
411 methods³⁶. Briefly, ESCs were initially cultured in primed ESC (pESC) media consisting of KnockOut
412 DMEM (Gibco#10829-018), fetal bovine serum (Gibco#A5209501), KnockOut serum replacement
413 (Invitrogen#10828-028), Glutamax (Gibco#35050-061), Anti-Anti (Gibco#15240-062), MEM Non-essential
414 amino acids (Gibco#11140-050), and beta-mercaptoethanol (Sigma#M7522). They were then transitioned
415 into ground-state, "naïve" ESCs (nESCs) by culturing for four passages in N2B27 media containing
416 DMEM/F12 (Gibco#11330-032), Neurobasal media (Gibco#21103-049), Gluamax, Anti-Anti, N2 sup-
417 plement (Invitrogen#17502048), and B27 supplement without vitamin A (Invitrogen#12587-010), and
418 beta-mercaptoethanol. Both pESC and nESC media were supplemented with 3 μ M GSK3 inhibitor
419 CHIR99021 (Sigma #SML1046-5MG), 1 μ M MEK inhibitor PD0325901 (Sigma #PZ0162-5MG), and 1,000
420 units/mL leukemia inhibitory factor (LIF, Millipore#ESG1107).

421 nESCs were differentiated into epiblast-like cells (EpiLCs, 48 hours) and extendend EpiLCs (exEpiLCs,
422 96 hours) by culturing in N2B27 media containing DMEM/F12, Neurobasal media, Gluamax, Anti-Anti,
423 N2 supplement, B27 supplement (Invitrogen#17504044), beta-mercaptoethanol, fibroblast growth factor 2
424 (FGF2, R&D Biotechne 233-FB), and activin A (R&D Biotechne 338AC050CF), as previously described³⁶.

425 **RNA sequencing (RNA-seq)**

426 After ensuring read quality via FastQC (v0.11.8), reads were then mapped to the mm10 *Mus musculus*
427 genome (Gencode) using STAR (v2.5.3a), during which we removed duplicates and kept only uniquely
428 mapped reads. Count files were generated by FeatureCounts (Subread v1.5.0), and BAM files were
429 converted to bigwigs using deeptools (v3.1.3) and visualized by the UCSC genome browser. RStudio (v3.6.0)
430 was then used to analyze counts files by DESeq2 (v1.26.0)²² to identify differentially expressed genes
431 (DEGs) with a q-value (p-adjusted via FDR/Benjamini–Hochberg correction) less than 0.1 and a log2 fold
432 change greater than 0.5. For all DESeq2 analyses, log2 fold changes were calculated with IfcShrink using
433 the ashR package⁸⁷. MA-plots were generated by ggpahr (v0.6.0), and Eulerr diagrams were generated by
434 eulerr (v6.1.1). Boxplots and scatterplots were generated by ggpahr (v0.6.0) and ggplot2 (v3.3.2). The Upset
435 plot was generated via the package UpSetR (v1.4.0)⁸⁸. Gene ontology (GO) analyses were performed by
436 the R package enrichPlot (v1.16.2) using the biological processes setting and compareCluster.

437 **Chromatin immunoprecipitation followed by DNA sequencing (ChIP-seq)**

438 ChIP-seq reads were aligned to mm10 using Bowtie1 (v1.1.2) allowing up to two mismatches. Only
439 uniquely mapped reads were used for analysis. Peaks were called using MACS2 software (v2.2.9.1) using
440 input BAM files for normalization, with filters for a q-value < 0.1 and a fold enrichment > 1. We removed
441 “black-listed” genomic regions that often give aberrant signals. Common peak sets were obtained in R via
442 DiffBind (v3.6.5). In the case of KDM5C ChIP-seq, *Kdm5c*-KO peaks were then subtracted from wild-type
443 samples using bedtools (v2.25.0). Peak proximity to genome annotations was determined by ChIPSeeker
444 (v1.32.1). Gene ontology (GO) analyses were performed by the R package enrichPlot (v1.16.2) using the
445 biological processes setting and compareCluster. Enriched motifs were identified using HOMER⁵⁸. Average
446 binding across the genome was visualized using deeptools (v3.1.3). Bigwigs were visualized using the
447 UCSC genome browser.

448 **CpG island (CGI) analysis**

449 Locations of CpG islands were determined through the mm10 UCSC genome browser CpG island track.
450 CGI coordinates were then annotated using ChIPseeker (v1.32.1) and filtered for promoters of germline
451 genes (TSS ± 500).

452 **Whole genome bisulfite sequencing (WGBS)**

453 Genomic DNA (gDNA) from naïve ESCs and extended EpiLCs was extracted using the Wizard Genomic
454 DNA Purification Kit (Promega A1120), following the instructions for Tissue Culture Cells. gDNA from
455 two wild-types and two *Kdm5c*-KOs of each cell type was sent to Novogene for WGBS using the Illumina
456 NovaSeq X Plus platform and sequenced for 150bp paired-end reads (PE150). Reads were adapter and
457 quality trimmed with Trim Galore (v0.6.10) and aligned to the mm10 genome using Bismark (v0.22.1).
458 Analysis of differential methylation at germline gene promoters was performed using methylKit (v1.28.0) with a
459 minimum coverage of 3 paired reads, a percentage cut-off of 25%, and q-value of 0.01. Average percentage
460 methylation at germline gene promoters was determined via methylKit (v1.28.0). Methylation bedgraph
461 tracks were generated via Bismark and visualized using the UCSC genome browser.

462 **Data availability**

463 **Published datasets**

464 All published datasets are available at the Gene Expression Omnibus (GEO) <https://www.ncbi.nlm.nih>
465 .gov/geo. Published RNA-seq datasets analyzed in this study included the male wild-type and *Kdm5c*-KO
466 adult amygdala and hippocampus²⁰ (available at GEO: GSE127722) and male wild-type and *Kdm5c*-KO
467 EpiLCs⁴¹ (available at GEO: GSE96797).

468 Previously published ChIP-seq experiments included KDM5C in wild-type and *Kdm5c*-KO EpiLCs⁴¹ (avail-
469 able at GEO: GSE96797) and mouse primary neuron cultures (PNCs) from the cortex and hippocampus¹²
470 (available at GEO: GSE61036). ChIP-seq of histone 3 lysine 4 dimethylation in male wild-type and *Kdm5c*-KO
471 EpiLCs⁴¹ is also available at GEO: GSE96797. ChIP-seq of histone 3 lysine 4 trimethylation in wild-type and
472 *Kdm5c*-KO male amygdala²⁰ are available at GEO: GSE127817.

473 **Data analysis**

474 Scripts used to generate the results, tables, and figures of this study are available via a GitHub repository:
475 XXX

476 **Acknowledgements**

477 We thank Drs. Sundeep Kalantry, Milan Samanta, and Rebecca Malcore for providing protocols and
478 expertise in culturing mouse ESCs and EpiLCs, as well as providing wild-type and *Kdm5c*-KO ESCs used in
479 this study. We thank Dr. Jacob Mueller for his insight in germline gene regulation and directing us to the
480 germline-depleted mouse models. We also thank Drs. Stephanie Bielas, Michael Sutton, Donna Martin, and
481 the members of the Iwase, Sutton, Bielas, and Martin labs for helpful discussions and critiques of the data.
482 We thank members of the University of Michigan Reproductive Sciences Program for providing feedback
483 throughout the development of this work. This work was supported by grants from the National Institutes
484 of Health (NIH) (National Institute of Neurological Disorders and Stroke: NS089896, 5R21NS104774, and
485 NS116008 to S.I.), Farrehi Family Foundation Grant (to S.I.), the University of Michigan Career Training in
486 Reproductive Biology (NIH T32HD079342, to K.M.B), and the NIH Early Stage Training in the Neurosciences
487 Training Grant (T32-NS076401 to K.M.B).

488 **Author contributions**

489 K.M.B. and S.I. conceived the study and designed the experiments. I.V. generated the ESC and exEpiLC
490 WGBS data. K.M.B performed the data analysis and all other experiments. K.M.B and S.I. wrote and edited
491 the manuscript.

492 **References**

- 493 1. Strahl, B.D., and Allis, C.D. (2000). The language of covalent histone modifications. *Nature* **403**,
494 41–45. <https://doi.org/10.1038/47412>.

- 495 2. Jenuwein, T., and Allis, C.D. (2001). Translating the Histone Code. *Science* *293*, 1074–1080.
496 <https://doi.org/10.1126/science.1063127>.
- 497 3. Lewis, E.B. (1978). A gene complex controlling segmentation in *Drosophila*. *Nature* *276*, 565–570.
498 <https://doi.org/10.1038/276565a0>.
- 499 4. Kennison, J.A., and Tamkun, J.W. (1988). Dosage-dependent modifiers of polycomb and antennapedia
500 mutations in *Drosophila*. *Proc. Natl. Acad. Sci. U.S.A.* *85*, 8136–8140. <https://doi.org/10.1073/pnas.85.21.8136>.
- 501 5. Kassis, J.A., Kennison, J.A., and Tamkun, J.W. (2017). Polycomb and Trithorax Group Genes in
502 *Drosophila*. *Genetics* *206*, 1699–1725. <https://doi.org/10.1534/genetics.115.185116>.
- 503 6. Gabriele, M., Lopez Tobon, A., D'Agostino, G., and Testa, G. (2018). The chromatin basis of
504 neurodevelopmental disorders: Rethinking dysfunction along the molecular and temporal axes. *Prog
Neuropsychopharmacol Biol Psychiatry* *84*, 306–327. <https://doi.org/10.1016/j.pnpbp.2017.12.013>.
- 505 7. Schaefer, A., Sampath, S.C., Intrator, A., Min, A., Gertler, T.S., Surmeier, D.J., Tarakhovsky, A.,
506 and Greengard, P. (2009). Control of cognition and adaptive behavior by the GLP/G9a epigenetic
507 suppressor complex. *Neuron* *64*, 678–691. <https://doi.org/10.1016/j.neuron.2009.11.019>.
- 508 8. Iwase, S., Lan, F., Bayliss, P., De La Torre-Ubieta, L., Huarte, M., Qi, H.H., Whetstine, J.R., Bonni, A.,
509 Roberts, T.M., and Shi, Y. (2007). The X-Linked Mental Retardation Gene SMCX/JARID1C Defines a
510 Family of Histone H3 Lysine 4 Demethylases. *Cell* *128*, 1077–1088. <https://doi.org/10.1016/j.cell.2007.02.017>.
- 511 9. Claes, S., Devriendt, K., Van Goethem, G., Roelen, L., Meireleire, J., Raeymaekers, P., Cassiman,
512 J.J., and Fryns, J.P. (2000). Novel syndromic form of X-linked complicated spastic paraparesis. *Am J
Med Genet* *94*, 1–4.
- 513 10. Jensen, L.R., Amende, M., Gurok, U., Moser, B., Gimmel, V., Tzschach, A., Janecke, A.R., Tariverdian,
514 G., Chelly, J., Fryns, J.P., et al. (2005). Mutations in the JARID1C gene, which is involved in
transcriptional regulation and chromatin remodeling, cause X-linked mental retardation. *Am J Hum
Genet* *76*, 227–236. <https://doi.org/10.1086/427563>.
- 515 11. Carmignac, V., Nambot, S., Lehalle, D., Callier, P., Moortgat, S., Benoit, V., Ghoumid, J., Delobel,
516 B., Smol, T., Thuillier, C., et al. (2020). Further delineation of the female phenotype with KDM5C
disease causing variants: 19 new individuals and review of the literature. *Clin Genet* *98*, 43–55.
<https://doi.org/10.1111/cge.13755>.
- 515 12. Iwase, S., Brookes, E., Agarwal, S., Badeaux, A.I., Ito, H., Vallianatos, C.N., Tomassy, G.S., Kasza, T.,
Lin, G., Thompson, A., et al. (2016). A Mouse Model of X-linked Intellectual Disability Associated with
Impaired Removal of Histone Methylation. *Cell Reports* *14*, 1000–1009. <https://doi.org/10.1016/j.celrep.2015.12.091>.

- 517 13. Scandaglia, M., Lopez-Atalaya, J.P., Medrano-Fernandez, A., Lopez-Cascales, M.T., Del Blanco, B.,
Lipinski, M., Benito, E., Olivares, R., Iwase, S., Shi, Y., et al. (2017). Loss of Kdm5c Causes Spurious
Transcription and Prevents the Fine-Tuning of Activity-Regulated Enhancers in Neurons. *Cell Rep* **21**,
518 47–59. <https://doi.org/10.1016/j.celrep.2017.09.014>.
- 519 14. Devlin, D.K., Ganley, A.R.D., and Takeuchi, N. (2023). A pan-metazoan view of germline-soma
distinction challenges our understanding of how the metazoan germline evolves. *Current Opinion in
520 Systems Biology* **36**, 100486. <https://doi.org/10.1016/j.coisb.2023.100486>.
- 521 15. Lehmann, R. (2012). Germline Stem Cells: Origin and Destiny. *Cell Stem Cell* **10**, 729–739.
<https://doi.org/10.1016/j.stem.2012.05.016>.
- 522 16. Endoh, M., Endo, T.A., Shinga, J., Hayashi, K., Farcas, A., Ma, K.W., Ito, S., Sharif, J., Endoh, T.,
Onaga, N., et al. (2017). PCGF6-PRC1 suppresses premature differentiation of mouse embryonic
523 stem cells by regulating germ cell-related genes. *eLife* **6**. <https://doi.org/10.7554/eLife.21064>.
- 524 17. Mochizuki, K., Sharif, J., Shirane, K., Uranishi, K., Bogutz, A.B., Janssen, S.M., Suzuki, A., Okuda,
A., Koseki, H., and Lorincz, M.C. (2021). Repression of germline genes by PRC1.6 and SETDB1
in the early embryo precedes DNA methylation-mediated silencing. *Nat Commun* **12**, 7020. <https://doi.org/10.1038/s41467-021-27345-x>.
- 525 18. Velasco, G., Hubé, F., Rollin, J., Neuillet, D., Philippe, C., Bouzinba-Segard, H., Galvani, A., Viegas-
Péquignot, E., and Francastel, C. (2010). Dnmt3b recruitment through E2F6 transcriptional repressor
mediates germ-line gene silencing in murine somatic tissues. *Proc Natl Acad Sci U S A* **107**, 9281–
526 9286. <https://doi.org/10.1073/pnas.1000473107>.
- 527 19. Hackett, J.A., Reddington, J.P., Nestor, C.E., Dunican, D.S., Branco, M.R., Reichmann, J., Reik,
W., Surani, M.A., Adams, I.R., and Meehan, R.R. (2012). Promoter DNA methylation couples
528 genome-defence mechanisms to epigenetic reprogramming in the mouse germline. *Development*
139, 3623–3632. <https://doi.org/10.1242/dev.081661>.
- 529 20. Vallianatos, C.N., Raines, B., Porter, R.S., Bonefas, K.M., Wu, M.C., Garay, P.M., Collette, K.M.,
Seo, Y.A., Dou, Y., Keegan, C.E., et al. (2020). Mutually suppressive roles of KMT2A and KDM5C
in behaviour, neuronal structure, and histone H3K4 methylation. *Commun Biol* **3**, 278. <https://doi.org/10.1038/s42003-020-1001-6>.
- 530 21. Li, B., Qing, T., Zhu, J., Wen, Z., Yu, Y., Fukumura, R., Zheng, Y., Gondo, Y., and Shi, L. (2017). A
Comprehensive Mouse Transcriptomic BodyMap across 17 Tissues by RNA-seq. *Sci Rep* **7**, 4200.
531 <https://doi.org/10.1038/s41598-017-04520-z>.
- 532 22. Love, M.I., Huber, W., and Anders, S. (2014). Moderated estimation of fold change and dispersion for
533 RNA-seq data with DESeq2. *Genome Biol* **15**, 550. <https://doi.org/10.1186/s13059-014-0550-8>.

- 537 23. Crackower, M.A., Kolas, N.K., Noguchi, J., Sarao, R., Kikuchi, K., Kaneko, H., Kobayashi, E., Kawai, Y.,
Kozieradzki, I., Landers, R., et al. (2003). Essential Role of Fkbp6 in Male Fertility and Homologous
538 Chromosome Pairing in Meiosis. *Science* *300*, 1291–1295. <https://doi.org/10.1126/science.1083022>.
- 539 24. Xiol, J., Cora, E., Koglgruber, R., Chuma, S., Subramanian, S., Hosokawa, M., Reuter, M., Yang, Z.,
Berninger, P., Palencia, A., et al. (2012). A Role for Fkbp6 and the Chaperone Machinery in piRNA
540 Amplification and Transposon Silencing. *Molecular Cell* *47*, 970–979. <https://doi.org/10.1016/j.molcel.2012.07.019>.
- 541 25. Cheng, S., Altmeppen, G., So, C., Welp, L.M., Penir, S., Ruhwedel, T., Menelaou, K., Harasimov, K.,
Stützer, A., Blayney, M., et al. (2022). Mammalian oocytes store mRNAs in a mitochondria-associated
542 membraneless compartment. *Science* *378*, eabq4835. <https://doi.org/10.1126/science.abq4835>.
- 543 26. Rouland, A., Masson, D., Lagrost, L., Vergès, B., Gautier, T., and Bouillet, B. (2022). Role of
apolipoprotein C1 in lipoprotein metabolism, atherosclerosis and diabetes: A systematic review.
544 *Cardiovasc Diabetol* *21*, 272. <https://doi.org/10.1186/s12933-022-01703-5>.
- 545 27. Leduc, V., Jasmin-Bélanger, S., and Poirier, J. (2010). APOE and cholesterol homeostasis in
Alzheimer's disease. *Trends in Molecular Medicine* *16*, 469–477. <https://doi.org/10.1016/j.molmed.2010.07.008>.
- 546 28. Mueller, J.L., Skaletsky, H., Brown, L.G., Zaghlul, S., Rock, S., Graves, T., Auger, K., Warren,
W.C., Wilson, R.K., and Page, D.C. (2013). Independent specialization of the human and mouse X
547 chromosomes for the male germ line. *Nat Genet* *45*, 1083–1087. <https://doi.org/10.1038/ng.2705>.
- 548 29. Handel, M.A., and Eppig, J.J. (1979). Sertoli Cell Differentiation in the Testes of Mice Genetically
Deficient in Germ Cells. *Biology of Reproduction* *20*, 1031–1038. <https://doi.org/10.1095/biolreprod20.5.1031>.
- 549 30. Green, C.D., Ma, Q., Manske, G.L., Shami, A.N., Zheng, X., Marini, S., Moritz, L., Sultan, C.,
Gurczynski, S.J., Moore, B.B., et al. (2018). A Comprehensive Roadmap of Murine Spermatogenesis
Defined by Single-Cell RNA-Seq. *Dev Cell* *46*, 651–667.e10. <https://doi.org/10.1016/j.devcel.2018.07.025>.
- 550 31. Soh, Y.Q., Junker, J.P., Gill, M.E., Mueller, J.L., van Oudenaarden, A., and Page, D.C. (2015). A
Gene Regulatory Program for Meiotic Prophase in the Fetal Ovary. *PLoS Genet* *11*, e1005531.
551 <https://doi.org/10.1371/journal.pgen.1005531>.
- 552 32. Magnúsdóttir, E., and Surani, M.A. (2014). How to make a primordial germ cell. *Development* *141*,
245–252. <https://doi.org/10.1242/dev.098269>.
- 553 33. Günesdogan, U., Magnúsdóttir, E., and Surani, M.A. (2014). Primordial germ cell specification: A
context-dependent cellular differentiation event [corrected]. *Philos Trans R Soc Lond B Biol Sci* *369*.
554 <https://doi.org/10.1098/rstb.2013.0543>.

- 559 34. Bardot, E.S., and Hadjantonakis, A.-K. (2020). Mouse gastrulation: Coordination of tissue patterning,
specification and diversification of cell fate. *Mechanisms of Development* *163*, 103617. <https://doi.org/10.1016/j.mod.2020.103617>.
- 560
- 561 35. Hayashi, K., Ohta, H., Kurimoto, K., Aramaki, S., and Saitou, M. (2011). Reconstitution of the
mouse germ cell specification pathway in culture by pluripotent stem cells. *Cell* *146*, 519–532.
<https://doi.org/10.1016/j.cell.2011.06.052>.
- 562
- 563 36. Samanta, M., and Kalantry, S. (2020). Generating primed pluripotent epiblast stem cells: A methodol-
ogy chapter. *Curr Top Dev Biol* *138*, 139–174. <https://doi.org/10.1016/bs.ctdb.2020.01.005>.
- 564
- 565 37. Welling, M., Chen, H., Muñoz, J., Musheev, M.U., Kester, L., Junker, J.P., Mischerikow, N., Arbab, M.,
Kuijk, E., Silberstein, L., et al. (2015). DAZL regulates Tet1 translation in murine embryonic stem cells.
EMBO Reports *16*, 791–802. <https://doi.org/10.15252/embr.201540538>.
- 566
- 567 38. Macfarlan, T.S., Gifford, W.D., Driscoll, S., Lettieri, K., Rowe, H.M., Bonanomi, D., Firth, A., Singer, O.,
Trono, D., and Pfaff, S.L. (2012). Embryonic stem cell potency fluctuates with endogenous retrovirus
activity. *Nature* *487*, 57–63. <https://doi.org/10.1038/nature11244>.
- 568
- 569 39. Suzuki, A., Hirasaki, M., Hishida, T., Wu, J., Okamura, D., Ueda, A., Nishimoto, M., Nakachi, Y.,
Mizuno, Y., Okazaki, Y., et al. (2016). Loss of MAX results in meiotic entry in mouse embryonic and
germline stem cells. *Nat Commun* *7*, 11056. <https://doi.org/10.1038/ncomms11056>.
- 570
- 571 40. Borgel, J., Guibert, S., Li, Y., Chiba, H., Schübeler, D., Sasaki, H., Forné, T., and Weber, M. (2010).
Targets and dynamics of promoter DNA methylation during early mouse development. *Nat Genet* *42*,
1093–1100. <https://doi.org/10.1038/ng.708>.
- 572
- 573 41. Samanta, M.K., Gayen, S., Harris, C., Maclary, E., Murata-Nakamura, Y., Malcore, R.M., Porter, R.S.,
Garay, P.M., Vallianatos, C.N., Samollow, P.B., et al. (2022). Activation of Xist by an evolutionarily
conserved function of KDM5C demethylase. *Nat Commun* *13*, 2602. <https://doi.org/10.1038/s41467-022-30352-1>.
- 574
- 575 42. Koubova, J., Menke, D.B., Zhou, Q., Capel, B., Griswold, M.D., and Page, D.C. (2006). Retinoic
acid regulates sex-specific timing of meiotic initiation in mice. *Proc. Natl. Acad. Sci. U.S.A.* *103*,
2474–2479. <https://doi.org/10.1073/pnas.0510813103>.
- 576
- 577 43. Lin, Y., Gill, M.E., Koubova, J., and Page, D.C. (2008). Germ Cell-Intrinsic and -Extrinsic Factors
Govern Meiotic Initiation in Mouse Embryos. *Science* *322*, 1685–1687. <https://doi.org/10.1126/science.1166340>.
- 578
- 579 44. Endo, T., Mikedis, M.M., Nicholls, P.K., Page, D.C., and De Rooij, D.G. (2019). Retinoic Acid and Germ
Cell Development in the Ovary and Testis. *Biomolecules* *9*, 775. <https://doi.org/10.3390/biom9120775>.
- 580

- 581 45. Gupta, N., Yakhou, L., Albert, J.R., Azogui, A., Ferry, L., Kirsh, O., Miura, F., Battault, S., Yamaguchi,
582 K., Laisné, M., et al. (2023). A genome-wide screen reveals new regulators of the 2-cell-like cell state.
Nat Struct Mol Biol. <https://doi.org/10.1038/s41594-023-01038-z>.
- 583 46. Pohlers, M., Truss, M., Frede, U., Scholz, A., Strehle, M., Kuban, R.-J., Hoffmann, B., Morkel, M.,
Birchmeier, C., and Hagemann, C. (2005). A Role for E2F6 in the Restriction of Male-Germ-Cell-
584 Specific Gene Expression. Current Biology 15, 1051–1057. <https://doi.org/10.1016/j.cub.2005.04.060>.
- 585 47. Dahlet, T., Truss, M., Frede, U., Al Adhami, H., Bardet, A.F., Dumas, M., Vallet, J., Chicher, J.,
Hamann, P., Kottnik, S., et al. (2021). E2F6 initiates stable epigenetic silencing of germline genes
586 during embryonic development. Nat Commun 12, 3582. <https://doi.org/10.1038/s41467-021-23596-w>.
- 587 48. Agulnik, A.I., Mitchell, M.J., Mattei, M.G., Borsani, G., Avner, P.A., Lerner, J.L., and Bishop, C.E.
(1994). A novel X gene with a widely transcribed Y-linked homologue escapes X-inactivation in mouse
588 and human. Hum Mol Genet 3, 879–884. <https://doi.org/10.1093/hmg/3.6.879>.
- 589 49. Carrel, L., Hunt, P.A., and Willard, H.F. (1996). Tissue and lineage-specific variation in inactive
X chromosome expression of the murine Smcx gene. Hum Mol Genet 5, 1361–1366. <https://doi.org/10.1093/hmg/5.9.1361>.
- 590 50. Sheardown, S., Norris, D., Fisher, A., and Brockdorff, N. (1996). The mouse Smcx gene exhibits
developmental and tissue specific variation in degree of escape from X inactivation. Hum Mol Genet
592 5, 1355–1360. <https://doi.org/10.1093/hmg/5.9.1355>.
- 593 51. Xu, J., Deng, X., and Disteche, C.M. (2008). Sex-Specific Expression of the X-Linked Histone
Demethylase Gene Jarid1c in Brain. PLoS ONE 3, e2553. <https://doi.org/10.1371/journal.pone.0002553>.
- 594 52. Wang, P.J., McCarrey, J.R., Yang, F., and Page, D.C. (2001). An abundance of X-linked genes
expressed in spermatogonia. Nat Genet 27, 422–426. <https://doi.org/10.1038/86927>.
- 595 53. Khil, P.P., Smirnova, N.A., Romanienko, P.J., and Camerini-Otero, R.D. (2004). The mouse X
chromosome is enriched for sex-biased genes not subject to selection by meiotic sex chromosome
598 inactivation. Nat Genet 36, 642–646. <https://doi.org/10.1038/ng1368>.
- 599 54. Hurlin, P.J. (1999). Mga, a dual-specificity transcription factor that interacts with Max and contains a
T-domain DNA-binding motif. The EMBO Journal 18, 7019–7028. <https://doi.org/10.1093/emboj/18.2.7019>.
- 600 55. Tatsumi, D., Hayashi, Y., Endo, M., Kobayashi, H., Yoshioka, T., Kiso, K., Kanno, S., Nakai, Y., Maeda,
I., Mochizuki, K., et al. (2018). DNMTs and SETDB1 function as co-repressors in MAX-mediated
repression of germ cell-related genes in mouse embryonic stem cells. PLoS ONE 13, e0205969.
602 <https://doi.org/10.1371/journal.pone.0205969>.

- 603 56. Stielow, B., Finkernagel, F., Stiewe, T., Nist, A., and Suske, G. (2018). MGA, L3MBTL2 and E2F6
determine genomic binding of the non-canonical Polycomb repressive complex PRC1.6. *PLoS Genet*
604 14, e1007193. <https://doi.org/10.1371/journal.pgen.1007193>.
- 605 57. Tahiliani, M., Mei, P., Fang, R., Leonor, T., Rutenberg, M., Shimizu, F., Li, J., Rao, A., and Shi, Y.
(2007). The histone H3K4 demethylase SMCX links REST target genes to X-linked mental retardation.
606 *Nature* 447, 601–605. <https://doi.org/10.1038/nature05823>.
- 607 58. Heinz, S., Benner, C., Spann, N., Bertolino, E., Lin, Y.C., Laslo, P., Cheng, J.X., Murre, C., Singh, H.,
and Glass, C.K. (2010). Simple Combinations of Lineage-Determining Transcription Factors Prime
cis-Regulatory Elements Required for Macrophage and B Cell Identities. *Molecular Cell* 38, 576–589.
608 <https://doi.org/10.1016/j.molcel.2010.05.004>.
- 609 59. Gajiwala, K.S., Chen, H., Cornille, F., Roques, B.P., Reith, W., Mach, B., and Burley, S.K. (2000).
Structure of the winged-helix protein hRFX1 reveals a new mode of DNA binding. *Nature* 403,
610 916–921. <https://doi.org/10.1038/35002634>.
- 611 60. Swoboda, P., Adler, H.T., and Thomas, J.H. (2000). The RFX-Type Transcription Factor DAF-19
Regulates Sensory Neuron Cilium Formation in *C. elegans*. *Molecular Cell* 5, 411–421. [https://doi.org/10.1016/S1097-2765\(00\)80436-0](https://doi.org/10.1016/S1097-2765(00)80436-0).
- 612 61. Ashique, A.M., Choe, Y., Karlen, M., May, S.R., Phamluong, K., Solloway, M.J., Ericson, J., and
Peterson, A.S. (2009). The Rfx4 Transcription Factor Modulates Shh Signaling by Regional Control of
614 Ciliogenesis. *Sci. Signal.* 2. <https://doi.org/10.1126/scisignal.2000602>.
- 615 62. Kistler, W.S., Baas, D., Lemeille, S., Paschaki, M., Seguin-Estevez, Q., Barras, E., Ma, W., Duteyrat, J.-
L., Morlé, L., Durand, B., et al. (2015). RFX2 Is a Major Transcriptional Regulator of Spermiogenesis.
616 *PLoS Genet* 11, e1005368. <https://doi.org/10.1371/journal.pgen.1005368>.
- 617 63. Wu, Y., Hu, X., Li, Z., Wang, M., Li, S., Wang, X., Lin, X., Liao, S., Zhang, Z., Feng, X., et al.
(2016). Transcription Factor RFX2 Is a Key Regulator of Mouse Spermiogenesis. *Sci Rep* 6, 20435.
618 <https://doi.org/10.1038/srep20435>.
- 619 64. Liu, M., Zhu, Y., Xing, F., Liu, S., Xia, Y., Jiang, Q., and Qin, J. (2020). The polycomb group protein
PCGF6 mediates germline gene silencing by recruiting histone-modifying proteins to target gene
620 promoters. *J Biol Chem* 295, 9712–9724. <https://doi.org/10.1074/jbc.RA119.012121>.
- 621 65. Otani, J., Nankumo, T., Arita, K., Inamoto, S., Ariyoshi, M., and Shirakawa, M. (2009). Structural basis
for recognition of H3K4 methylation status by the DNA methyltransferase 3A ATRX–DNMT3–DNMT3L
622 domain. *EMBO Reports* 10, 1235–1241. <https://doi.org/10.1038/embor.2009.218>.
- 623 66. Guo, X., Wang, L., Li, J., Ding, Z., Xiao, J., Yin, X., He, S., Shi, P., Dong, L., Li, G., et al. (2015).
Structural insight into autoinhibition and histone H3-induced activation of DNMT3A. *Nature* 517,
624 640–644. <https://doi.org/10.1038/nature13899>.

- 625 67. Meissner, A., Mikkelsen, T.S., Gu, H., Wernig, M., Hanna, J., Sivachenko, A., Zhang, X., Bernstein, B.E., Nusbaum, C., Jaffe, D.B., et al. (2008). Genome-scale DNA methylation maps of pluripotent and
626 differentiated cells. *Nature* **454**, 766–770. <https://doi.org/10.1038/nature07107>.
- 627 68. Nassar, L.R., Barber, G.P., Benet-Pagès, A., Casper, J., Clawson, H., Diekhans, M., Fischer, C., Gonzalez, J.N., Hinrichs, A.S., Lee, B.T., et al. (2023). The UCSC Genome Browser database: 2023
628 update. *Nucleic Acids Research* **51**, D1188–D1195. <https://doi.org/10.1093/nar/gkac1072>.
- 629 69. Akalin, A., Kormaksson, M., Li, S., Garrett-Bakelman, F.E., Figueiroa, M.E., Melnick, A., and Mason,
630 C.E. (2012). methylKit: A comprehensive R package for the analysis of genome-wide DNA methylation
profiles. *Genome Biol* **13**, R87. <https://doi.org/10.1186/gb-2012-13-10-r87>.
- 631 70. Torres-Padilla, M.-E. (2020). On transposons and totipotency. *Philos Trans R Soc Lond B Biol Sci*
632 **375**, 20190339. <https://doi.org/10.1098/rstb.2019.0339>.
- 633 71. Yang, M., Yu, H., Yu, X., Liang, S., Hu, Y., Luo, Y., Izsvák, Z., Sun, C., and Wang, J. (2022). Chemical-
induced chromatin remodeling reprograms mouse ESCs to totipotent-like stem cells. *Cell Stem Cell*
634 **29**, 400–418.e13. <https://doi.org/10.1016/j.stem.2022.01.010>.
- 635 72. Zhang, J., Zhang, M., Acampora, D., Vojtek, M., Yuan, D., Simeone, A., and Chambers, I. (2018).
OTX2 restricts entry to the mouse germline. *Nature* **562**, 595–599. <https://doi.org/10.1038/s41586-018-0581-5>.
- 637 73. Long, H.K., King, H.W., Patient, R.K., Odom, D.T., and Klose, R.J. (2016). Protection of CpG
islands from DNA methylation is DNA-encoded and evolutionarily conserved. *Nucleic Acids Res* **44**,
638 6693–6706. <https://doi.org/10.1093/nar/gkw258>.
- 639 74. Weber, M., Hellmann, I., Stadler, M.B., Ramos, L., Pääbo, S., Rebhan, M., and Schübeler, D. (2007).
Distribution, silencing potential and evolutionary impact of promoter DNA methylation in the human
640 genome. *Nat Genet* **39**, 457–466. <https://doi.org/10.1038/ng1990>.
- 641 75. Al Adhami, H., Vallet, J., Schaal, C., Schumacher, P., Bardet, A.F., Dumas, M., Chicher, J., Hammann,
P., Daujat, S., and Weber, M. (2023). Systematic identification of factors involved in the silencing
of germline genes in mouse embryonic stem cells. *Nucleic Acids Research* **51**, 3130–3149. <https://doi.org/10.1093/nar/gkad071>.
- 643 76. Aubert, Y., Egolf, S., and Capell, B.C. (2019). The Unexpected Noncatalytic Roles of Histone Modifiers
in Development and Disease. *Trends in Genetics* **35**, 645–657. <https://doi.org/10.1016/j.tig.2019.06.004>.
- 644 77. Morgan, M.A.J., and Shilatifard, A. (2020). Reevaluating the roles of histone-modifying enzymes
and their associated chromatin modifications in transcriptional regulation. *Nat Genet* **52**, 1271–1281.
646 <https://doi.org/10.1038/s41588-020-00736-4>.

- 647 78. Abidayeva, K., Berbée, J.F.P., Blokland, A., Jansen, P.J., Hoek, F.J., Meijer, O., Lütjohann, D., Gautier, T., Pillot, T., De Vente, J., et al. (2008). Human apolipoprotein C-I expression in mice impairs learning and memory functions. *Journal of Lipid Research* 49, 856–869. <https://doi.org/10.1194/jlr.M700518JLR200>.
- 648
- 649 79. Nielsen, A.Y., and Gjerstorff, M.F. (2016). Ectopic Expression of Testis Germ Cell Proteins in Cancer and Its Potential Role in Genomic Instability. *Int J Mol Sci* 17. <https://doi.org/10.3390/ijms17060890>.
- 650
- 651 80. Adebayo Babatunde, K., Najafi, A., Salehipour, P., Modarressi, M.H., and Mobasher, M.B. (2017). Cancer/Testis genes in relation to sperm biology and function. *Iranian Journal of Basic Medical Sciences* 20. <https://doi.org/10.22038/ijbms.2017.9259>.
- 652
- 653 81. Janic, A., Mendizabal, L., Llamazares, S., Rossell, D., and Gonzalez, C. (2010). Ectopic expression of germline genes drives malignant brain tumor growth in *Drosophila*. *Science* 330, 1824–1827. <https://doi.org/10.1126/science.1195481>.
- 654
- 655 82. Ghafouri-Fard, S., and Modarressi, M.-H. (2012). Expression of Cancer–Testis Genes in Brain Tumors: Implications for Cancer Immunotherapy. *Immunotherapy* 4, 59–75. <https://doi.org/10.2217/imt.11.145>.
- 656
- 657 83. Bonefas, K.M., and Iwase, S. (2021). Soma-to-germline transformation in chromatin-linked neurodevelopmental disorders? *FEBS J*. <https://doi.org/10.1111/febs.16196>.
- 658
- 659 84. Velasco, G., Walton, E.L., Sterlin, D., Hédonin, S., Nitta, H., Ito, Y., Fouyssac, F., Mégarbané, A., Sasaki, H., Picard, C., et al. (2014). Germline genes hypomethylation and expression define a molecular signature in peripheral blood of ICF patients: Implications for diagnosis and etiology. *Orphanet J Rare Dis* 9, 56. <https://doi.org/10.1186/1750-1172-9-56>.
- 660
- 661 85. Walton, E.L., Francastel, C., and Velasco, G. (2014). Dnmt3b Prefers Germ Line Genes and Centromeric Regions: Lessons from the ICF Syndrome and Cancer and Implications for Diseases. *Biology* (Basel) 3, 578–605. <https://doi.org/10.3390/biology3030578>.
- 662
- 663 86. Samaco, R.C., Mandel-Brehm, C., McGraw, C.M., Shaw, C.A., McGill, B.E., and Zoghbi, H.Y. (2012). Crh and Oprm1 mediate anxiety-related behavior and social approach in a mouse model of MECP2 duplication syndrome. *Nat Genet* 44, 206–211. <https://doi.org/10.1038/ng.1066>.
- 664
- 665 87. Stephens, M. (2016). False discovery rates: A new deal. *Biostat*, kxw041. <https://doi.org/10.1093/biostatistics/kxw041>.
- 666
- 667 88. Conway, J.R., Lex, A., and Gehlenborg, N. (2017). UpSetR: An R package for the visualization of intersecting sets and their properties. *Bioinformatics* 33, 2938–2940. <https://doi.org/10.1093/bioinformatics/btx364>.
- 668

669 **Figures and Tables**

- 670 • Supplementary table 1: list of all germline genes.
- 671 – Columns to include:
- 672 * KDM5C bound vs not
- 673 * Log2fc in EpiLC, brain (separate columns?)
- 674 – CGI vs non

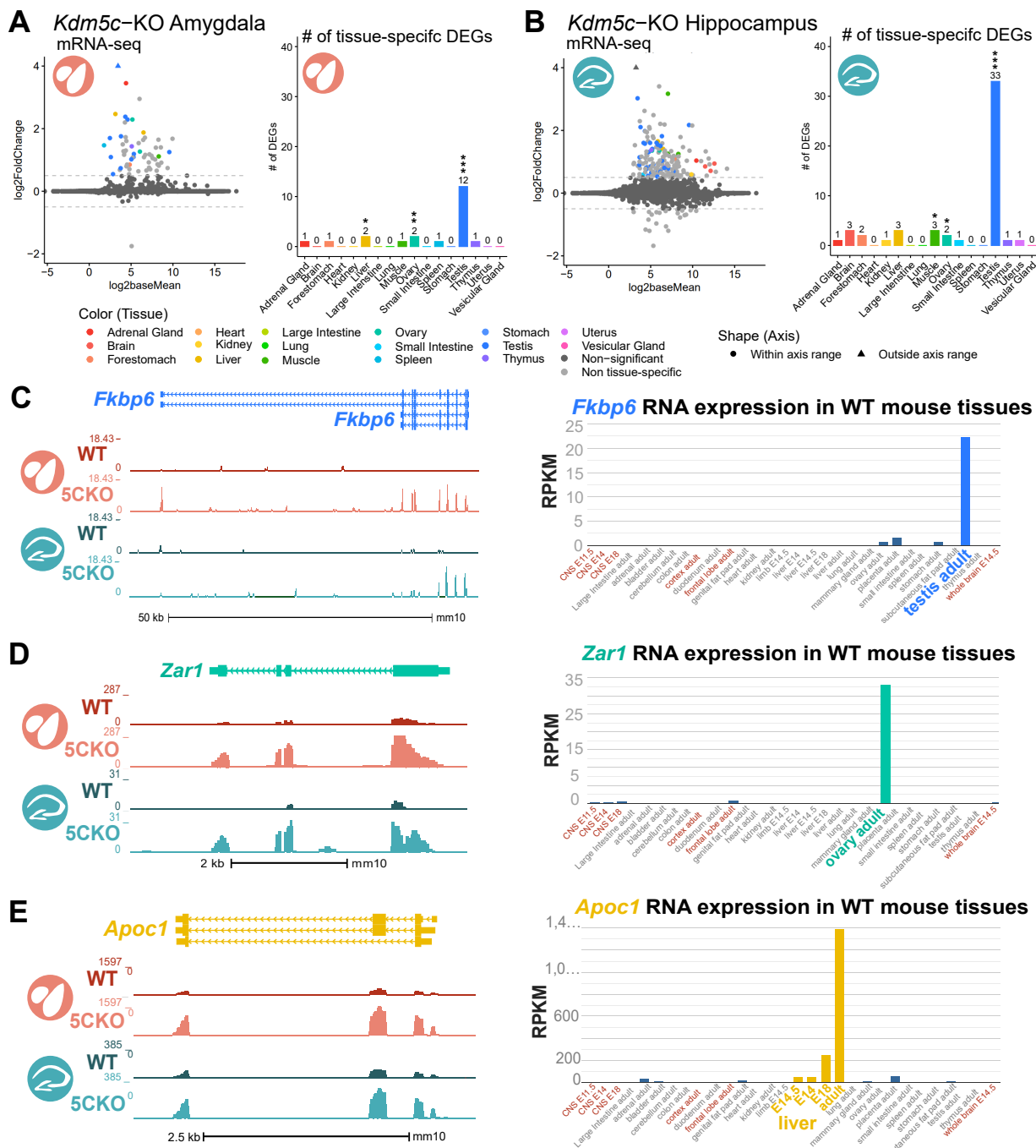


Figure 1: Tissue-enriched genes are misexpressed in the *Kdm5c*-KO brain. **A-B.** Expression of tissue-enriched genes (Li et al 2017) in the male *Kdm5c*-KO amygdala (A) and hippocampus (B). Left - MA plot of mRNA-sequencing. Right - Number of tissue-enriched differentially expressed genes (DEGs). * $p < 0.05$, ** $p < 0.01$, *** $p < 0.001$, Fisher's exact test. **C.** Left - Average bigwigs of an example aberrantly expressed testis-enriched DEG, *FK506 binding protein 6* (*Fkbp6*) in the wild-type (WT) and *Kdm5c*-KO (5CKO) amygdala (red) and hippocampus (teal). Right - Expression of *Cyct* in wild-type tissues from NCBI Gene, with testis highlighted in blue and brain tissues highlighted in red. **D.** Left - Average bigwigs of an example ovary-enriched DEG, *Zygotic arrest 1* (*Zar1*). Right - Expression of *Zar1* in wild-type tissues from NCBI Gene, with ovary highlighted in teal and brain tissues highlighted in red. **E.** Left - Average bigwigs of an example liver-enriched DEG, *Apolipoprotein C-I* (*Apoc1*). Right - Expression of *Apoc1* in wild-type tissues from NCBI Gene, with liver highlighted in orange and brain tissues highlighted in red.

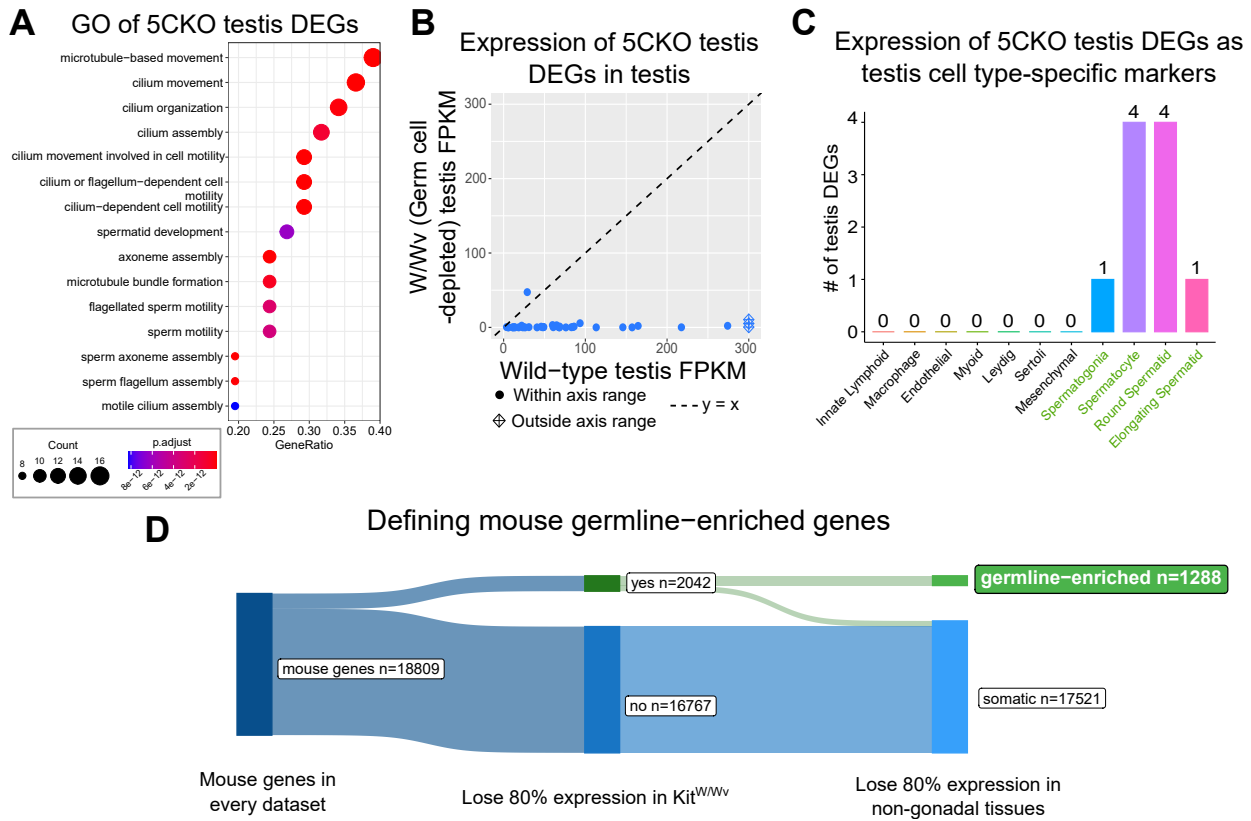


Figure 2: Aberrant transcription of germline genes in the *Kdm5c*-KO in the brain. **A.** enrichPlot gene ontology (GO) of *Kdm5c*-KO amygdala and hippocampus testis-enriched DEGs **B.** Expression of testis DEGs in wild-type (WT) testis versus germ cell-depleted (W/W_v) testis (Mueller et al 2013). Expression is in Fragments Per Kilobase of transcript per Million mapped reads (FPKM). **C.** Number of testis DEGs that were classified as cell-type specific markers in a single cell RNA-seq dataset of the testis (Green et al 2018). Germline cell types are highlighted in green, somatic cell types in black. **D.** Sankey diagram of mouse genes filtered for germline enrichment based on their expression in wild-type and germline-depleted mice and in adult mouse non-gonadal tissues (Li et al 2017).

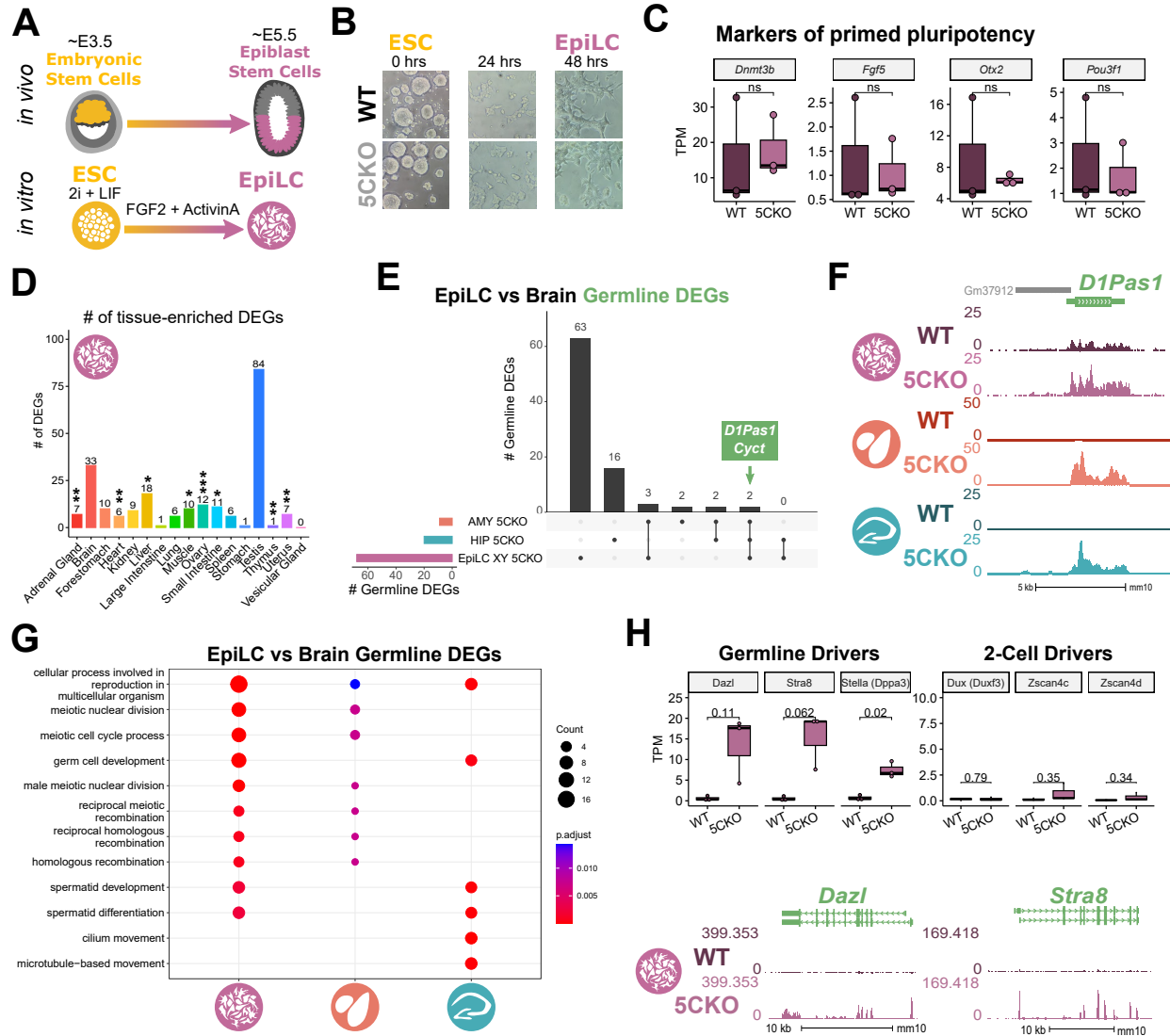


Figure 3: *Kdm5c*-KO epiblast-like cells express key drivers of germline identity

A. Top - Diagram of *in vivo* differentiation of embryonic stem cells (ESCs) of the inner cell mass into epiblast stem cells. Bottom - *in vitro* differentiation of ESCs into epiblast-like cells (EpiLCs).

B. Representative images of wild-type (WT) and *Kdm5c*-KO cells during ESC to EpiLC differentiation. Brightfield images taken at 20X.

C. No significant difference in primed pluripotency marker expression in wild-type versus *Kdm5c*-KO EpiLCs. Welch's t-test, expression in transcripts per million (TPM).

D. Number of tissue-enriched differentially expressed genes (DEGs) in *Kdm5c*-KO EpiLCs. * $p<0.05$, ** $p<0.01$, *** $p<0.001$, Fisher's exact test.

E. Upset plot displaying the overlap of germline DEGs expressed in *Kdm5c*-KO EpiLCs, amygdala (AMY), and hippocampus (HIP) RNA-seq datasets.

F. Average bigwigs of an example germline gene, *D1Pas1*, that is dysregulated *Kdm5c*-KO EpiLCs (top, purple), amygdala (middle, red), and hippocampus (bottom, blue).

G. enrichPlot gene ontology analysis comparing enriched biological processes for *Kdm5c*-KO EpiLC, amygdala, and hippocampus germline DEGs.

H. Top left - Example germline identity DEGs unique to EpiLCs. Top right - Example 2-cell genes that are not dysregulated in *Kdm5c*-KO EpiLCs. Bottom - Average bigwigs of *Dazl* and *Stra8* expression in wild-type and *Kdm5c*-KO EpiLCs.

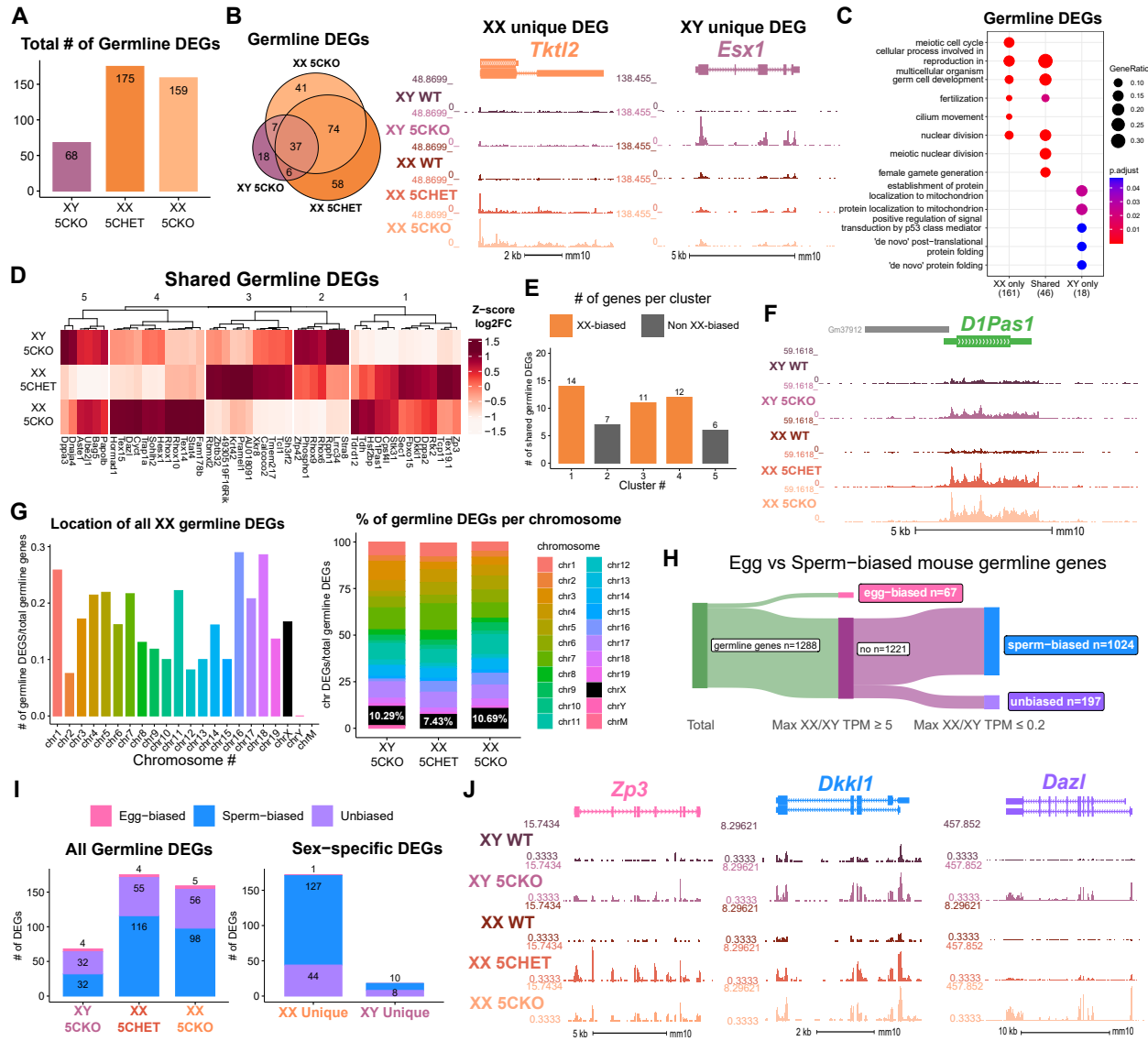


Figure 4: Chromosomal sex influences *Kdm5c*-KO germline gene misexpression. **A.** Total number of germline-enriched RNA-seq DEGs for male hemizygous *Kdm5c* knockout EpilCs (XY 5CKO, purple), female heterozygous *Kdm5c* knockout (XX 5CHET, orange), female homozygous *Kdm5c* knockout (XX 5CKO, light orange) EpilCs. **B.** Left - Eulerr overlap of *Kdm5c* mutant male and female EpilC germline DEGs. Right - Example of germline DEGs unique to females or males, *Tktl2* and *Esx1*. **C.** enrichPlot gene ontology analysis comparing enriched biological processes for germline DEGs shared between *Kdm5c* mutant males and females (Shared), or unique to one sex (XX only or XY only). **D.** Heatmap of germline DEGs shared between male and female mutants. Color is the average log 2 fold change from sex-matched wild-type. **E.** Number of genes within each cluster from D. Clusters with higher expression in females compared to males (XX-biased) highlighted in orange. **F.** Example average bigwigs of a male and female shared germline DEG *D1Pas1* that is more highly expressed in female mutants. **G.** Left - Number of all female germline DEGs located on each chromosome over the total number of germline-enriched genes on that chromosome. Right - Percentage of germline DEGs that lie on each chromosome for each *Kdm5c* mutant. X chromosome highlighted in black. **H.** Sankey diagram classifying egg-biased (pink) and sperm-biased (blue) and unbiased (purple) mouse germline-enriched genes. **I.** Number of egg, sperm, or unbiased germline DEGs for male and female *Kdm5c* mutants. **J.** Example bigwigs of egg-biased (*Zp3*), sperm-biased (*Dkk1*), and unbiased (*Dazl*) germline genes dysregulated in both male and female *Kdm5c* mutants.

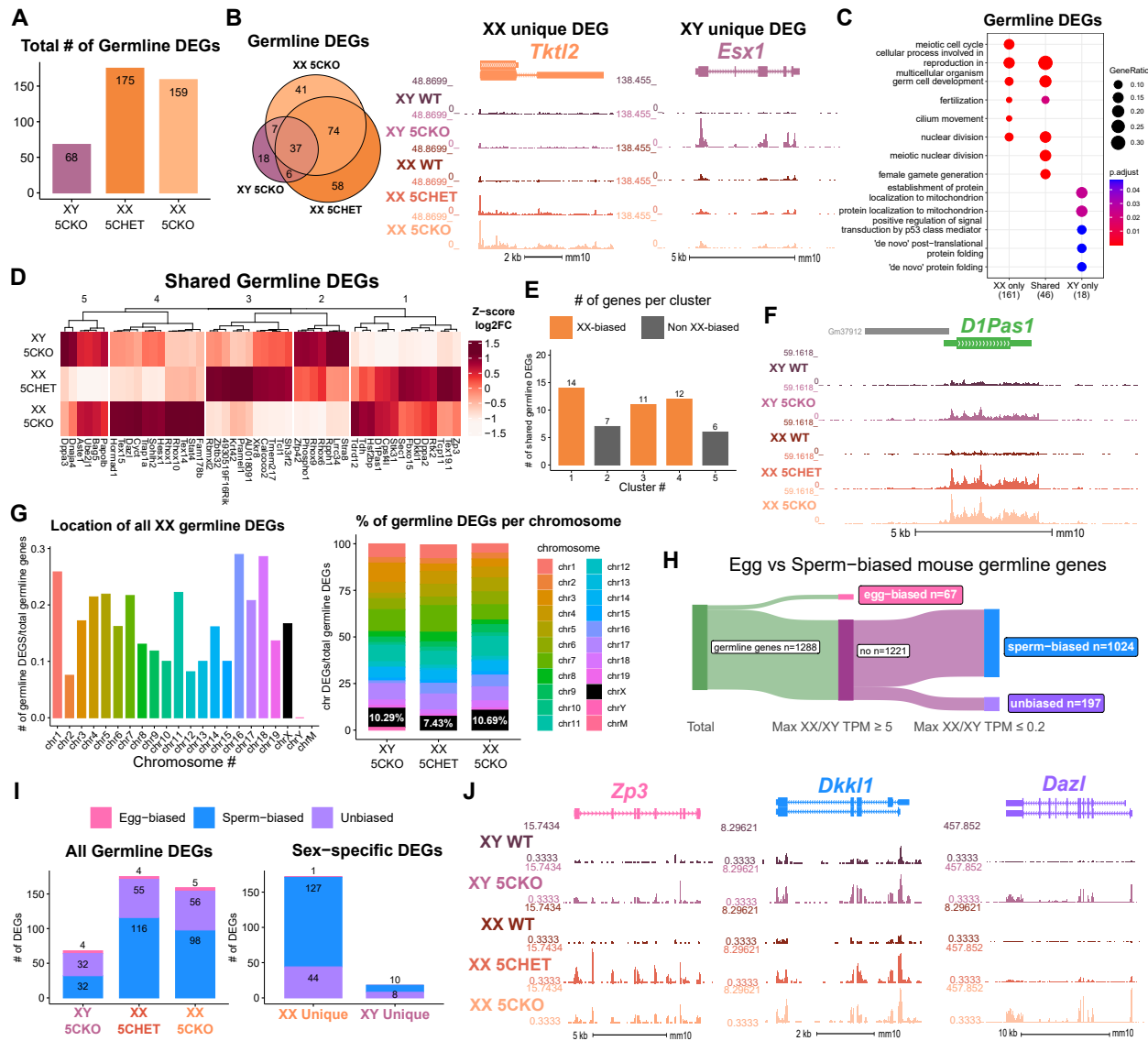


Figure 5: Chromosomal sex influences *Kdm5c*-KO germline gene misexpression. **A.** Total number of germline-enriched RNA-seq DEGs for male hemizygous *Kdm5c* knockout EpilCs (XY 5CKO, purple), female heterozygous *Kdm5c* knockout (XX 5CHET, orange), female homozygous *Kdm5c* knockout (XX 5CKO, light orange) EpilCs. **B.** Left - Eulerr overlap of *Kdm5c* mutant male and female EpilC germline DEGs. Right - Example of germline DEGs unique to females or males, *Tktl2* and *Esx1*. **C.** enrichPlot gene ontology analysis comparing enriched biological processes for germline DEGs shared between *Kdm5c* mutant males and females (Shared), or unique to one sex (XX only or XY only). **D.** Heatmap of germline DEGs shared between male and female mutants. Color is the average log2 fold change from sex-matched wild-type. **E.** Number of genes within each cluster from D. Clusters with higher expression in females compared to males (XX-biased) highlighted in orange. **F.** Example average bigwigs of a male and female shared germline DEG *D1Pas1* that is more highly expressed in female mutants. **G.** Left - Number of all female germline DEGs located on each chromosome over the total number of germline-enriched genes on that chromosome. Right - Percentage of germline DEGs that lie on each chromosome for each *Kdm5c* mutant. X chromosome highlighted in black. **H.** Sankey diagram classifying egg-biased (pink) and sperm-biased (blue) and unbiased (purple) mouse germline-enriched genes. **I.** Number of egg, sperm, or unbiased germline DEGs for male and female *Kdm5c* mutants. **J.** Example bigwigs of egg-biased (*Zp3*), sperm-biased (*Dkk1*), and unbiased (*Dazl*) dysregulated in both male and female *Kdm5c* mutants.

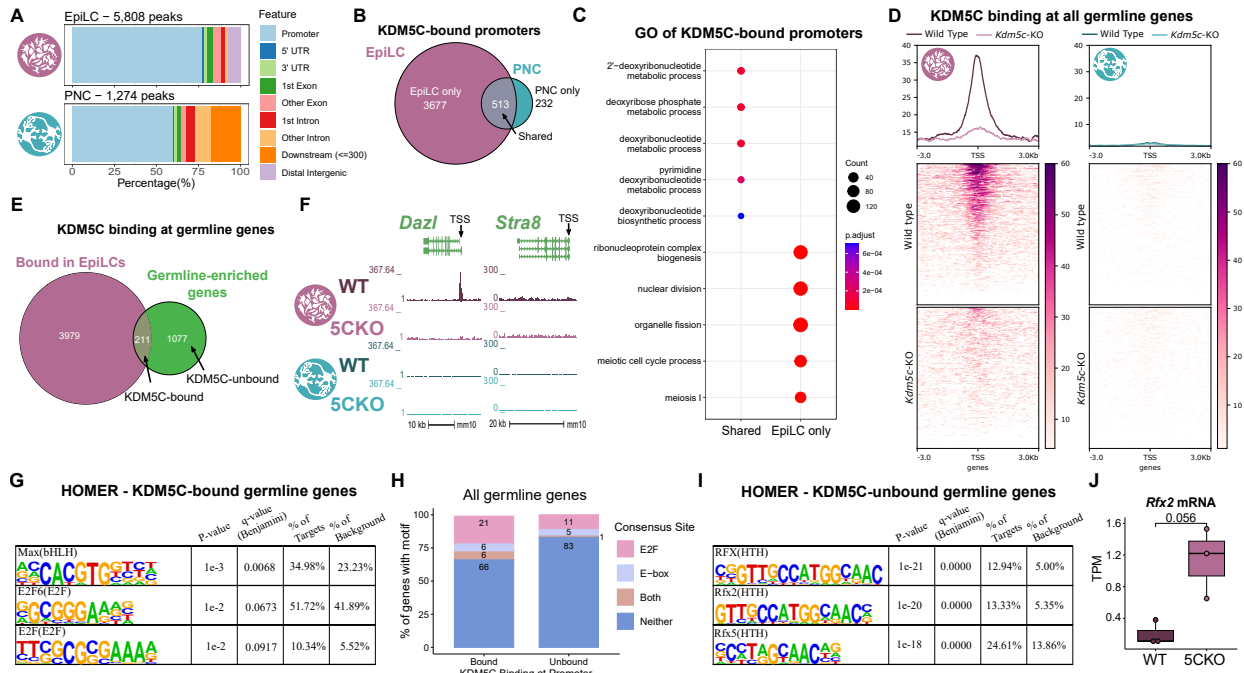


Figure 6: KDM5C binds to a subset of germline gene promoters during early embryogenesis. **A.** ChIPseeker localization of KDM5C peaks at different genomic regions in EpiLCs (top) and hippocampal and cortex primary neuron cultures (PNCs, bottom). **B.** Overlap of genes with KDM5C bound to their promoters ($TSS \pm 500$) in EpiLCs (purple) and PNCs (blue). **C.** Gene ontology (GO) comparison of genes with KDM5C bound to their promoter in EpiLCs and PNCs. Genes were classified as either bound in EpiLCs only (EpiLC only), unique to PNCs (PNC only, no significant ontologies) or bound in both PNCs and EpiLCs (Shared). **D.** Average KDM5C binding around the transcription start site (TSS) of all germline-enriched genes in EpiLCs (left) and PNCs (right). **E.** Eulerr of number of germline-enriched genes (green) with significant KDM5C binding at their promoter in EpiLCs (purple). **F.** Example KDM5C ChIP-seq bigwigs of KDM5C binding at the *Dazl* TSS but not *Stra8* in EpiLCs. **G.** HOMER motif analysis of all KDM5C-bound germline gene promoters, highlighting significant enrichment of MAX, E2F6, and E2F motifs. **H.** Number of all gene promoters bound or unbound by KDM5C with instances of the E2F or E-box consensus sequence. **I.** HOMER motif analysis of all KDM5C-unbound germline gene promoters, highlighting significant enrichment of RFX family transcription factor motifs. **J.** Expression of RNA-seq DEG *Rfx2* in wild-type and *Kdm5c*-KO EpiLCs. P-value of Welch's t-test, expression in transcripts per million (TPM).

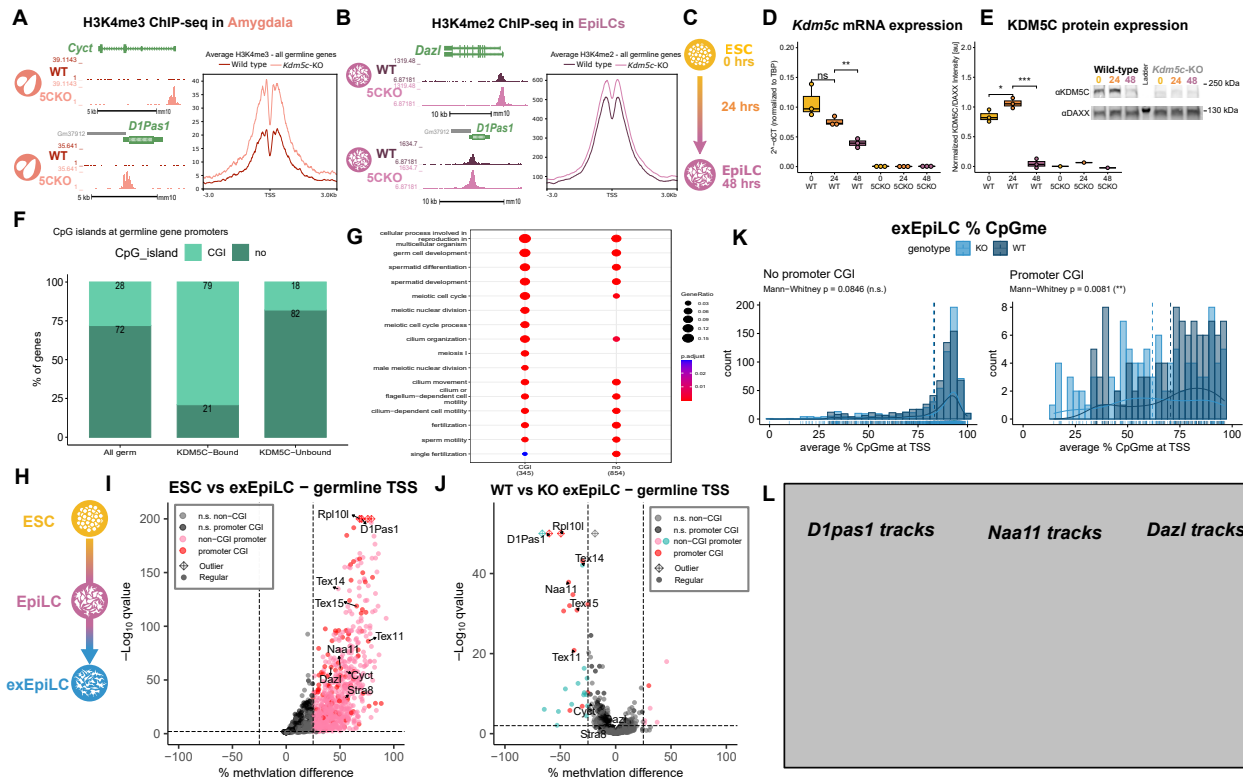


Figure 7: KDM5C's catalytic activity promotes long-term silencing of germline genes via DNA methylation. **A.** Left - Bigwigs of representative histone 3 lysine 4 trimethylation (H3K4me3) ChIP-seq peaks at two germline genes in the wild-type (WT) and *Kdm5c*-KO (5CKO) adult amygdala. Right - Average H3K4me3 at the transcription start site (TSS) of all germline-enriched genes in wild-type (dark red) and *Kdm5c*-KO (light red) amygdala. **B.** Left - Bigwigs of representative histone 3 lysine 4 dimethylation (H3K4me2) ChIP-seq peaks at representative germline genes in wild-type and *Kdm5c*-KO EpiLCs. Right - Average H3K4me2 at the TSS of all germline-enriched genes in wild-type (dark purple) and *Kdm5c*-KO (light purple) EpiLCs. **C.** Diagram of embryonic stem cell (ESC) to epiblast-like cell (EpiLC) differentiation protocol and collection time points for RNA and protein. **D.** Real time quantitative PCR (RT-qPCR) of *Kdm5c* mRNA expression, calculated in comparison to TBP expression ($2^{-\Delta\Delta CT}$). * $p < 0.05$, ** $p < 0.01$, *** $p < 0.001$, Welch's t-test. **E.** KDM5C protein expression normalized to DAXX. Quantified intensity using ImageJ (artificial units - au). Right - representative lanes of Western blot for KDM5C and DAXX. * $p < 0.05$, ** $p < 0.01$, *** $p < 0.001$, Welch's t-test. **F.** Percentage of germline genes that harbor CpG islands (CGIs) in their promoters, based on UCSC annotation. Comparing all germline-enriched genes, KDM5C-bound germline genes, or KDM5C-unbound germline genes. **G.** enrichPlot gene ontology analysis of CGI-promoter versus non-CGI promoter germline genes. **H.** Diagram of ESC to extended EpiLC (exEpiLC) differentiation. **I.** Volcano plot of whole genome bisulfite sequencing (WGBS) comparing CpG methylation at germline gene promoters ($TSS \pm 500$) in wild-type ESCs versus exEpiLCs. Promoter CGI genes highlighted in red, hypermethylated genes lacking a promoter CGI in pink. **J.** Volcano plot of WGBS of wild-type versus *Kdm5c*-KO exEpiLCs. Promoter CGI genes highlighted in red, hypermethylated genes lacking a promoter CGI in blue, hypomethylated genes lacking a promoter CGI in blue. **K.** Example UCSC browser shots of germline genes of CpG methylation (CpGme) in wild-type and *Kdm5c*-KO ESCs and exEpiLCs. **L.** Histogram of average percent CpGme at the promoter for germline genes with or without promoter CGIs. Wild-type in navy and *Kdm5c*-KO in light blue. Dashed lines are average methylation for each genotype, p-values for Mann-Whitney U test.